AD-A044 681 BINARY SYSTEMS INC SILVER SPRING MD F/G 20/4
MAXIMUM-LIKELIHOOD FLOW-SPEED ESTIMATION.(U)
MAY 77 S GARDNER, F L REES N00014-72-C-0318
UNCLASSIFIED WB77-1 NL

1 OF 1
AD A044681

END
DATE FILMED
10-77
DDC

AD A044681

Binary Systems Inc.

(12)

Binary Systems Inc.

10750 Columbia Pike, Silver Spring, Md. 20901 (301) 593-2960

"MAXIMUM-LIKELIHOOD FLOW-SPEED ESTIMATION [redacted]

BY S. GARDNER
AND
F.L. REES

MAY 24, 1977

BINARY SYSTEMS, INC.
REPORT NO. WB77-1

PREPARED UNDER CONTRACT NO. N00014-72-C-0318

FOR THE

SENSOR TECHNOLOGY PROGRAM, CODE 222
OFFICE OF NAVAL RESEARCH
800 N. QUINCY STREET
ARLINGTON, VIRGINIA 22217

ATTENTION: MR. H. FITZPATRICK

ABSTRACT:

The design formulae and theoretical performance of a maximum-likelihood estimator for towed-array flow-speed estimation are discussed. Under appropriate conditions, it is shown that a maximum-likelihood estimate of convection velocity (which is related to tow speed) is achieved by performing a cross correlation between the outputs of two streamwise-separated flush-mounted surface probe hydrophones. The estimate, then, is derived by seeking the time delay which maximizes the cross correlation.

Conditions are examined consistent with achieving accurate speed determination to within a fraction of a knot. Fortuitously, the method derived has the property that, as speed is increased, both the level and bandwidth of the pressure signals increase, thus providing increased signal-to-noise ratio and more accurate time-delay information.

It is suggested that a confidence-level measurement, comparing the space-time correlation function derived from the data with a theoretical model, could be used to indicate flow anomalies. These flow anomalies might be attributable to disturbances such as flow separation. In such case, the device could be used also to sense flow stability.

Two implementations are discussed: one using a DElay Line TIme Compressor (DELTIC) and serial processing; the other using Shift Registers (SR) and parallel processing. A trade-off of serial faster-than-real-time DELTIC processing speed requirements

against the high degree of parallel processing needed with the SR approach is discussed.

A recommendation is made to design, build, and test such a speed estimation/stability sensor on standard towed arrays. It further is suggested that empirical results and experience thus derived could be extrapolated, along with a study of available other array surface pressure coherency data, to determine the feasibility of building such a sensor for non-standard towed array application.

1.0 INTRODUCTION:

The report discusses the design and performance of a maximum-likelihood estimator for towed-array flow-speed estimation. It is shown that, under appropriate conditions, the maximum-likelihood estimator consists of a correlator which measures the time delay corresponding to the peak of the broadband correlation measured between the outputs of two streamwise-separated flush-mounted surface probe hydrophones.

The hydrophones have a circular sensing surface, a small fraction of an inch in diameter, and respond primarily to the high-wavenumber, convective pressures produced by the turbulent boundary layer. The probes are separated longitudinally by a fraction of an inch, so that over most of the operating band the coherence is high.

This method of flow-speed estimation is capable of accurate speed determination to within a fraction of a knot. It has the desirable feature that, as speed is increased, both the level and bandwidth of the pressure signals increase, providing increased signal-to-noise ratio and more accurate time-delay information.

If disturbances such as flow separation exist in the vicinity of the surface probes, it is expected that erratic results will be obtained. Therefore, it is possible that this device also can be used to indicate flow stability. However, this subject requires further study.

It should be pointed out that, prior to use at sea, the speed-measurement system must be calibrated in a water tunnel. The calibration is expected to depend to some extent upon the location of the sensors within the towed array (since macroscale properties of the flow may change). In addition, since the relation between convective and flow speeds will change with speed (for a fixed system operating bandwidth), it will be necessary to calibrate the system over the entire operating speed range.

Originally this system was conceived for application to standard towed arrays. However, it may be possible that a similar system can be designed for speed and flow-stability estimation on other arrays. The technology exists today for building such sensors. It is likely that, with some types of towed arrays, the turbulent boundary layer will exhibit greater sensitivity to tow-point and flow dynamics than a standard array.

In addition, the report derives the estimation accuracy to be theoretically anticipated from a maximum-likelihood estimate of convection velocity. The errors perturbing the estimation accuracy are treated in two categories: a) bias errors; and b) fluctuation errors. The bias errors are residual errors causing a departure of the average of the estimate of the convection velocity from its true value. The fluctuation error is one of zero expectation whose rms value measures the dispersion of the estimates around their mean. It is, in part due to background noise corrupting the estimate. Additionally, in as much as the Turbulent

Boundary Layer (TBL) pressure fluctuations are noiselike, a residual fluctuation error occurs when the estimate is performed over a finite number of independent samples.

The report considers the functional dependence of these errors on the space-time correlative nature of both the TBL and background noise fluctuations, signal-to-noise ratio, and the number of independent samples used in estimating the correlation function. Design formulae indicating the dependence of the precision on each of the variables are developed. In addition, timing and time-resolution requirements are established consistent with the number of independent samples needed and the required precision.

Two fundamentally different implementations are discussed: one using a DElay Line TIme Compressor (DELTIC) and serial processing; the other using Shift-Registers (SR) and parallel processing. It is shown that a clocking rate of the order of hundreds of MHz is needed with the DELTIC to cover the whole speed range. The SR implementation leads to a far more modest clocking rate at the expense a high degree of parallel processing (of the order of 100 channels). However, it is suggested that the SR implementation is compatible with state-of-the-art LSI technology.

The report also discusses a scheme for deriving a measure of confidence level to be attributed to the estimate of convection velocity. This confidence-level measure is derived by

comparing estimates obtained from measured data with stored models of the TBL correlation structure. As such, a low confidence level would be indicative of a radical departure from the models. This departure then would indicate the presence of flow anomalies. Moreover, comparison of confidence levels derived with a non-standard array against similar measurements with a standard array could indicate the adequacy of extrapolating the TBL models to the non-standard array geometry; wherein, greater sensitivity to tow-point and flow dynamics might be anticipated.

The report recommends that available surface-pressure coherence data for non-standard arrays be studied to determine the feasibility of building a speed-estimation/flow-stability sensor for application to them. Some of the experience necessary for this step could be acquired through measurements made with a similar sensor applied to standard arrays.

2.0 CONCLUSIONS AND RECOMMENDATIONS:

It is concluded that an estimate of the TBL convection velocity may be made with suitable precision by performing a Maximum Likelihood Estimate (MLE). The MLE requires that a sampled-data estimate of the cross correlation between the forward- and the aft-hydrophone TBL-pressure signals be formed. In forming this cross correlation, the time series derived from the forward hydrophone is time-delayed to bring it to the point of maximum correlation with the aft hydrophone.

In order to improve the stability of the estimate of convection velocity, the TBL pressure fluctuations being a random process, multiple samples are needed. For the rms value of the fluctuations around the average estimator value to improve by being inversely proportional to the square-root of the number of samples, N, these time samples should be selected far enough apart in time so as to be decorrelated. Two partially correlated time series are being cross-correlated. Therefore, the requirement to achieve the full $1/\sqrt{N}$ improvement is that the space-time correlation coefficient of the TBL be small for the hydrophone separation, ξ, selected and for a total time separation equaling the time between samples minus that time delay, τ, which maximizes the cross correlation. A 5-millisecond interval between samples is suggested for free-stream velocities down to 8 kts.

It further is shown that the rms error of the estimator is inversely proportional to an equivalent angular-frequency bandwidth, $[(2\pi f_0)^2 + (1/3)(\pi W)^2]^{1/2}$, and the hydrophone separation, ξ. Here, W is the observation bandwidth, centered around a frequency f_0. In fact, this improvement is offset by another factor equal to unity plus the exponential of 1.4 times the Strouhal number $\xi f_0/U_c$, ξ being the fore-and-aft separation of the hydrophones and U_c the convection velocity. As a result, a minimum fluctuation about the average of the estimator is shown to occur at a separation, ξ_{opt}, equal to 1.584 hydrodynamic wavelengths (i.e., to 1.584 U_c/f_0). This restriction enforces separations of the order of 5×10^{-3}m(~0.2") at free-stream velocities of the order of 16 kts.

Additionally it is shown that the estimator rms fluctuations decrease with the Signal-to-Noise (Power) Ratio (SNR), γ, being directly proportional to $(1+\gamma^{-1})$. Moreover, the average of the estimator exhibits a slight bias error (i.e., its statistical average is not equal to the true value) for low SNR and a small number of samples. Typically, an SNR of 100 is adequate to remove the bias error and ensure a negligible contribution to the flucturation error. However, for the fluctuation error to be acceptably small, say 1% of the maximum velocity, at least 1000 independent samples would be needed. These would take 5 seconds to accumulate and this determines the time constant of the velocity sensor in response to changes in velocity. The 1000 independent samples are shown to be more than adequate to make the bias error insignificant.

It is apparent, from the theoretical analysis, that the MLE of convection velocity provides an estimation accuracy exceeding that implied by the Cramer-Rao bound. This anomaly appears to be real, and probably has its roots in the non-regular nature of the TBL space-time function assumed; which is attributed to Bakewell [2]. Indeed, Cramer [3] shows an example where non-regularity can lead to abnormally high precision. Swerling [4] has pointed out similar anomalies, and associates them with a tighter bound acquired through a procedure due to Barankin. (cf Swerling loc. cit. and Glove [5]) Be that as it may, the MLE does lead to a useful and intuitively satisfying procedure for estimating the convection velocity. The errors predicted also have a heuristic explanation. Therefore, it is suspected that it is the Cramer-Rao bound which is not tight enough for this non-regular case, and not that there are any deficiencies with the MLE procedure.

It is recommended that in designing a velocity sensor, only a two-to-one range of velocity be spanned for one fixed hydrophone-pair separation and that the optimum separation of $1.584\ U_c/f_0$ be chosen for the geometric mean, $\sqrt{\min U_c \cdot \max U_c}$, of the velocity range.

To limit errors to values of the order of 1% up to 16 kts, the time-delay increments should be of the order of 10 microseconds. Two implementations are discussed: one, using a faster-than-real-time serial processing scheme centered around DElay Line TIme Compressors (DELTIC); the other, a real-time parallel

scheme using Shift Registers (SR). The DELTIC scheme, consistent with the 10-microsecond real-time resolution, necessitates clocking rates of the order of several hundred megahertz. For this reason, this approach is not recommended. By way of contrast, the SR scheme requires a 200-stage SR, with the last 100 stages tapped, running at a shift rate of 100 KHz. Beyond that, 100 parallel 1-bit multipliers and 100 parallel 10-bit up/down counters (reset every 5 seconds) would be needed; again operating at a clocking rate of 100 KHz. Modern LSI technology easily can accommodate this.

The SR approach can be made compatible with an LED, 4-digit, floating-point display of free-stream velocity. In addition, it can be made to provide a feature for displaying a confidence level. This would facilitate providing the display operator with an indication of any anomalous behavior of the axial flow along the towed array; for example, a velocity sensor near the tail of the array might be a good indicator of flow and, hence, array stability.

To derive a confidence-level measure, models of the clipped space-time correlation appropriate to each of the convection velocities associated with each correlator time-delay tap could be stored in a Read Only Memory (ROM). The model appropriate to the estimated velocity then would be accessed and compared through differencing either in a mean-square or absolute-value sense summed across the time-delay taps dispersed either side of the tap for the estimated velocity. A small

value of this measure would correspond to a high confidence level, say 9 on a scale of 0 to 9. Lower numbers corresponding to higher values of the measure would be an indication that the estimated cross-correlation function did not match well with the model.

It is recommended that a velocity sensor/flow-stability sensor be designed, built and tested on standard towed arrays. The resultant data could be reduced and compared with the theory over a wide range of tow speeds and sensor locations. It further is recommended that available surface-pressure coherence data for non-standard arrays be studied to determine the feasibility of building a speed-estimation/flow-stability sensor for applications to other than standard arrays.

3.0 TECHNICAL DISCUSSIONS:

In attempting to estimate the convection velocity associated with flow in the Turbulent Boundary Layer (TBL), it is assumed that measurements will be made with a pair of flush-mounted hydrophones separated along the longitudinal flow direction of a towed array. Each hydrophone should be small in its longitudinal spatial extent in order that sufficient time resolution of the pressure fluctuation might be achieved; see Corcos [1]. Moreover, their spatial separation should be small enough to preserve some degree of space-time correlation. In this respect, assuming that broad-band pressure fluctuation measurements will be made consistent with good time resolution, a model attributed to Bakewell [2] will be presumed.

One type of hydrophone, which would respond primarily to high-wavenumber, convective pressures produced by the TBL, could have a circular sensing surface. In order to sense flow distortion when an array angle-of-attack is involved, three sets of hydrophone pairs spaced at 0°, 120°, and 240°, respectively, around the circumference of the array appear to be appropriate. For speed sensing, each hydrophone pair should be located in a region of (quasi) spatially homogeneous and temporally stationary TBL flow over the towed array. In a location near the tail-end of the array, anomalous results caused by flow instabilities might be anticipated. Thus, the velocity sensor also might be used as a detector of flow instability.

It appears appropriate to consider performing a Maximum-Likelihood Estimate (MLE) of the convection velocity in lieu of attempting a Baysian Estimate (BE). The BE requires a priori and (error) cost information not readily available; whereas the MLE can be estimated assuming only knowledge of the appropriate multi-dimensional joint Probability Density Functions (PDF's). The MLE maximizes the probability of a correct decision (estimate), without regard for an incorrect decision (estimate) or its cost. However, in the absence of a priori and (error) cost information, the MLE represents the most acceptable alternative. In order that a sufficiently smooth estimate of the convection velocity may be derived, multiple time samples are needed; gathered at time intervals separated enough to provide uncorrelated samples in a time series extracted from each hydrophone of the pair. Of course, correlation

must be maintained between the time series if the convection velocity is to be deduced. In this study, consistent with low implementation complexity and expense, spatial smoothing achieved by using more than two hydrophones will not be considered.

In order to investigate the form of the MLE, it will be assumed that the small flush-mounted hydrophones measure the pressure fluctuations dominated by the convective energy of the TBL. The only corrupting term to be considered will be broad-band extraneous noise. Inasmuch as the noise may be caused by sources which exhibit spatial correlation over the small distance separating the hydrophone pair, this possibility will be considered in deriving the MLE.

The broadband nature of the signals caused by the TBL pressure fluctuations also the noise fluctuations favors using a real rather than an analytic signal representation. The observed time series derived from the forward hydrophone in the TBL flow stream is given by

$$\underline{X}\left(x^{(F)},t\right) = \underline{P}\left(x^{(F)},t\right) + \underline{N}\left(x^{(F)},t\right);$$

likewise, from the aft hydrophone

$$\underline{X}\left(x^{(A)},t\right) = \underline{P}\left(x^{(A)},t\right) + \underline{N}\left(x^{(A)},t\right).$$

The quantities $x^{(F)}$ and $x^{(A)}$ are the spatial locations along the axial direction of the center of the forward hydrophone and aft hydrophone respectively. The quantities $t=t^{(F)}$ and $t=t^{(A)}$ are the times at which the time samples are derived from each of the forward and aft hydrophones respectively. Indeed, N time samples are derived in each of the time series at times $t_1^{(F)},\ldots,t_n^{(F)},\ldots,t_N^{(F)}$ for the forward hydrophone and $t_1^{(A)},\ldots,t_n^{(A)},\ldots,t_N^{(A)}$ for the aft hydrophone respectively. This notation will be contracted to

$$\underline{X}^{(F)} = \underline{P}^{(F)} + \underline{N}^{(F)}$$

and

$$\underline{X}^{(A)} = \underline{P}^{(A)} + \underline{N}^{(A)};$$

where the bar under each quantity indicates that it is a column vector N-tuple, and a superscript T transposes a column vector into row vector. Then,

$$\underline{X}^{(F)} = \begin{bmatrix} X_1^{(F)} \\ \cdot \\ \cdot \\ \cdot \\ X_N^{(F)} \end{bmatrix} , \quad \underline{X}^{(A)} = \begin{bmatrix} X_1^{(A)} \\ \cdot \\ \cdot \\ \cdot \\ X_N^{(A)} \end{bmatrix} ;$$

$$\underline{P}^{(F)} = \begin{bmatrix} P_1^{(F)} \\ \cdot \\ \cdot \\ \cdot \\ P_N^{(F)} \end{bmatrix} , \quad \underline{P}^{(A)} = \begin{bmatrix} P_1^{(A)} \\ \cdot \\ \cdot \\ \cdot \\ P_N^{(A)} \end{bmatrix} ;$$

also

$$\underline{N}^{(F)} = \begin{bmatrix} N_1^{(F)} \\ \cdot \\ \cdot \\ \cdot \\ N_N^{(F)} \end{bmatrix} , \quad \underline{N}^{(A)} = \begin{bmatrix} N_1^{(A)} \\ \cdot \\ \cdot \\ \cdot \\ N_N^{(A)} \end{bmatrix} .$$

Under the assumption that both the TBL pressure and noise fluctuations are Gaussianly distributed stochastic processes, the above formalism leads to a 2N-variable joint PDF conditional on the convection velocity U_c given by

$$W_{2N}\left(\underline{X}|U_c\right) = \left(2\pi\right)^{-N}\left[\det\left(\underline{\underline{R}}\right)\right]^{-1/2} \exp\left[-1/2\left(\underline{X}^T - \overline{\underline{X}}^T\right)\underline{\underline{R}}^{-1}\left(\underline{X}-\overline{\underline{X}}\right)\right]$$

In the PDF equation, the column vector $\underline{X}^{(F)}$ is adjoined as a subvector to the other sub-vector $\underline{X}^{(A)}$ so that

$$\underline{X} = \begin{bmatrix} \underline{X}^{(F)} \\ \\ \underline{X}^{(A)} \end{bmatrix} ;$$

also the bar over $\underline{X}$ indicates a statistical ensemble average (expected value) which is assumed to be zero for real representations

of the broad-band stochastic processes. The matrix $\underline{\underline{R}}$ is the correlation matrix which, because of the vanishing averages of $\underline{X}$, is the same as the covariance matrix. The matrix $\underline{\underline{R}}^{-1}$ is the inverse of $\underline{\underline{R}}$, also det $(\underline{\underline{R}})$ is the determinant of $\underline{\underline{R}}$. The correlation matrix $\underline{\underline{R}}$ is given by the expected value

$$\underline{\underline{R}} = \overline{\underline{X}\ \underline{X}^T}$$

$$= \begin{bmatrix} \overline{\underline{X}^{(F)}\ \underline{X}^{(F)T}} & \overline{\underline{X}^{(F)}\ \underline{X}^{(A)T}} \\ \overline{\underline{X}^{(A)}\ \underline{X}^{(F)T}} & \overline{\underline{X}^{(A)}\ \underline{X}^{(A)T}} \end{bmatrix}$$

This matrix has symmetric form. The submatrices in the $\underline{\underline{R}}$ matrix are given by the diagonal matrices

$$\overline{X^{(F)}\ X^{(F)T}} = \begin{bmatrix} \overline{X_1^{(F)\,2}} & & 0 \\ & \ddots & \\ 0 & & \overline{\left(X_N^{(F)}\right)^2} \end{bmatrix},$$

$$\overline{X^{(F)}\ X^{(A)T}} = \begin{bmatrix} \overline{X_1^{(F)}\ X_1^{(A)}} & & 0 \\ & \ddots & \\ 0 & & \overline{X_N^{(F)}\ X_N^{(A)}} \end{bmatrix},$$

$$\overline{\underline{X}^{(A)}\ \underline{X}^{(F)T}} = \begin{bmatrix} \overline{X_1^{(A)}\ X_1^{(F)}} & & 0 \\ & \ddots & \\ 0 & & \overline{X_N^{(A)}\ X_N^{(F)}} \end{bmatrix},$$

and

$$\overline{\underline{X}^{(A)}\ \underline{X}^{(A)^T}} = \begin{bmatrix} \overline{\left(X_1^{(A)}\right)^2} & & 0 \\ & \ddots & \\ 0 & & \overline{\left(X_N^{(A)}\right)^2} \end{bmatrix} \quad ;$$

where the diagonal form results from choosing the time samples sufficiently far apart so as to decorrelate them on both an intra- and interspatial-channel basis. Only the cross-correlation matrices $\overline{\underline{X}^{(F)}\ \underline{X}^{(A)^T}}$ and $\overline{\underline{X}^{(A)}\ \underline{X}^{(F)^T}}$ are functions of the convection velocity, U_c.

Invoking the previously mentioned spatial homogeniety and temporal stationarity, and exploiting the diagonal forms of the submatrices, leads to

$$W_{2N}\left(\underline{X}|U_c\right) = \prod_{n=1}^{N} \left[\frac{\exp\left\{ -\left[\left(X_n^{(F)}\right)^2 + \left(X_n^{(A)}\right)^2 - 2\rho_X X_n^{(F)} X_n^{(A)} \right] \Big/ 2\sigma_X^2 \left(1-\rho_X^2\right) \right\}}{2\pi\ \sigma_X^2 \left(1-\rho_X^2\right)^{1/2}} \right]$$

where

$$\overline{\left(X_1^{(F)}\right)^2} = \ldots\ldots\ldots = \overline{\left(X_N^{(F)}\right)^2} = \sigma_X^2 \quad ,$$

$$\overline{\left(X_1^{(A)}\right)^2} = \ldots\ldots\ldots = \overline{\left(X_N^{(A)}\right)^2} = \sigma_X^2$$

$$\overline{X_1^{(F)}\ X_1^{(A)}} = \ldots\ldots\ldots = \overline{X_N^{(F)}\ X_N^{(A)}} = \rho_X\ \sigma_X^2$$

also

$$\overline{X_1^{(A)}\ X_1^{(F)}} = \ldots\ldots\ldots = \overline{X_N^{(F)}\ X_N^{(A)}} = \rho_X\ \sigma_X^2 \ .$$

Again it should be noted that only ρ_X is a function of the convection velocity, U_c.

At this point, the general form of σ_X^2 and ρ_X should be evaluated. Under the spatial-homogeniety, temporal-stationarity assumptions, for any n=1,.....,N,

$$\sigma_X^2 = \overline{\left(X_n^{(F)}\right)^2}$$

$$= \overline{\left(P_n^{(F)} + N_n^{(F)}\right)^2}$$

$$= \sigma_P^2 + \sigma_N^2 \quad ,$$

likewise

$$\sigma_X^2 = \overline{\left(X_n^{(A)}\right)^2}$$

$$= \overline{\left(P_n^{(A)} + N_n^{(A)}\right)^2}$$

$$= \sigma_P^2 + \sigma_N^2 \quad .$$

Moreover,

$$\rho_X \sigma_X^2 = \overline{X_n^{(F)} X_n^{(A)}}$$

$$= \overline{\left(P_n^{(F)} + N_n^{(F)}\right)\left(P_n^{(A)} + N_n^{(A)}\right)}$$

$$= \rho_P \sigma_P^2 + \rho_N \sigma_N^2 \quad .$$

Therefore,

$$\rho_X = \frac{\rho_P \sigma_P^2 + \rho_N \sigma_N^2}{\sigma_P^2 + \sigma_N^2}$$

$$= \frac{\rho_P + \rho_N \left(\frac{\sigma_N}{\sigma_P}\right)^2}{1 + \left(\frac{\sigma_N}{\sigma_P}\right)^2} \quad .$$

Hence, the first central equation becomes

$$\rho_X = \frac{\left(\rho_P + \rho_N \gamma^{-1}\right)}{\left(1 + \gamma^{-1}\right)} ;$$

where

$$\gamma = \left(\frac{\sigma_P}{\sigma_N}\right)^2$$

is the Signal-to-Noise (Power) Ratio (SNR).

In order to derive an MLE of the convection velocity, U_c, a solution is sought to the equation

$$\frac{-\partial \log_e \left[W_{2N}\left(\underline{X} | U_c\right)\right]}{\partial U_c} = 0;$$

where $\log_e$ is the natural logarithm. This equation leads to

$$\frac{\partial}{\partial U_c}\left\{ \sum_{n=1}^{N} \frac{\left[\left(X_n^{(F)}\right)^2 + \left(X_n^{(A)}\right)^2 - 2\rho_X X_n^{(F)} X_n^{(A)}\right]}{2\sigma_X^2\left(1-\rho_X^2\right)} + \frac{N}{2} \log_e\left(1-\rho_X^2\right)\right\} = 0$$

Performing the partial differentiation and factoring out $\frac{\partial \rho_X}{\partial U_c}$ leads to

$$\left\{ \rho_X \sum_{n=1}^{N}\left[\left(X_n^{(F)}\right)^2 + \left(X_n^{(A)}\right)^2 - 2\rho_X X_n^{(F)} X_n^{(A)}\right] \right.$$

$$\left. - \left(1-\rho_X^2\right) \sum_{n=1}^{N} X_n^{(F)} X_n^{(A)} - N\rho_X\left(1-\rho_X^2\right)\sigma_X^2 \right\} \frac{\partial \rho_X}{\partial U_c} = 0$$

This leads to two solutions appearing as the second and third central equations; either

$$\frac{\partial \rho_X}{\partial U_c} = 0$$

or

$$\frac{1}{N}\sum_{n=1}^{N}\left[\left(X_n^{(F)}\right)^2+\left(X_n^{(A)}\right)^2-\left(\rho_X+\frac{1}{\rho_X}\right)X_n^{(F)}X_n^{(A)}\right]=\left(1-\rho_X{}^2\right)\sigma_X{}^2$$

The second central equation is not data-dependent. Therefore, it only indicates that, given a priori the form of the space-time correlation, the correct procedure to derive an MLE of U_c is to find the value of U_c where the correlation reaches a maximum. A minimum is not appropriate for the broad-band case. The third central equation is data-dependent.

The term $\frac{1}{N}\sum_{n=1}^{N}\left(X_n^{(F)}\right)^2$ is a consistent estimator of $\sigma_X{}^2$ (i.e., as $N\to\infty$ it converges in probability to $\sigma_X{}^2$). However, according to Cramer [3], it is not an unbiased estimator of $\sigma_X{}^2$. This biased property may be corrected by replacing the term $\frac{1}{N}\sum_{n=1}^{N}\left(X_n^{(F)}\right)^2$ by $\frac{1}{(N-1)}\sum_{n=1}^{N}\left(X_n^{(F)}\right)^2$; which is a consistent and unbiased estimator of $\sigma_X{}^2$, assuming the expected value of $X^{(F)}$ is zero. Likewise, by introducing a multiplication factor $\frac{N}{(N-1)}$ the estimators of the variance of $X^{(A)}$ and the covariance of $X^{(F)}X^{(A)}$ may be rendered both consistent and unbiased. Thus, the third central equation may be replaced by,

$$\frac{1}{(N-1)}\sum_{n=1}^{N}\left[\left(X_n^{(F)}\right)^2+\left(X_n^{(A)}\right)^2-\left(\rho_X+\frac{1}{\rho_X}\right)X_n^{(F)}X_n^{(A)}\right]=\frac{N}{(N-1)}\left(1-\rho_X{}^2\right)\sigma_X{}^2$$

Further, it is reasonable to introduce $\hat{\sigma}^2_{X|N}$ and $\hat{\rho}_{X|N}$ as the consistent and unbiased estimates of the variance and covariance, namely

$$\hat{\sigma}^2_{X|N}=\frac{1}{(N-1)}\sum_{n=1}^{N}\left(X_n^{(F)}\right)^2=\frac{1}{(N-1)}\sum_{n=1}^{N}\left(X_n^{(A)}\right)^2$$

and

$$\hat{\rho}_{X|N}\hat{\sigma}^2_{X|N}=\frac{1}{(N-1)}\sum_{n=1}^{N}X_n^{(F)}X_n^{(A)};$$

again under the assumption that the expected value of $X^{(F)}$ and $X^{(A)}$ are zero. In this way the third central equation may be compacted in the form

$$\hat{\rho}_{X|N}\hat{\sigma}^2_{X|N} = \frac{2(N-1)\hat{\sigma}^2_{X|N} - N\left(1-\rho_X^2\right)\sigma_X^2}{(N-1)\left(\rho_X + \frac{1}{\rho_X}\right)}$$

The expected value of the third central equation is

$$\overline{\hat{\rho}_{X|N}\hat{\sigma}^2_{X|N}} = \frac{2(N-1)\sigma_X^2 - N\left(1-\rho_X^2\right)\sigma_X^2}{(N-1)\left(\rho_X + \frac{1}{\rho_X}\right)} = \rho_X\sigma_X^2;$$

using the fact that

$$\overline{\hat{\rho}_{X|N}\hat{\sigma}_{X|N}}^2 = \rho_X\sigma_X^2.$$

The only way in which this equation can be satisfied exactly is if

$$\rho_X^2 = 1;$$

that is if

$$\rho_X = +1$$

or

$$\rho_X = -1;$$

in the case of broadband fluctuations only the first condition is appropriate. When this condition applies the fourth central equation becomes

$$\overline{\hat{\rho}_{X|N}\sigma^2_{X|N}} = \sigma_X^2$$

This condition implies that

$$\overline{\hat{\rho}_{X|N}} = \rho_X = 1,$$

which is consistent with the first central equation.

The condition for an MLE of U_c then is to apply a (usually gradient) search loop to locate the maximum of the estimate $\hat{\rho}_{X|N}$ of the TBL space-time correlation. In a bandwidth W arithmetically

centered around a frequency, f_0, Bakewell [2] has assumed that the TBL space-time correlation is given by a fifth central equation (shown in Figure 1)

$$\rho_p(\xi,\tau) = \exp\left[-0.7\left|\frac{\xi f_0}{U_c}\right|\right] \frac{\text{Sin } \pi W\left[\tau-\left(\xi/U_c\right)\right]}{\pi W\left[\tau-\left(\xi/U_c\right)\right]} \times \cos\left\{2\pi f_0\left[\tau-\left(\xi/U_c\right)\right]\right\} .$$

Here the Strouhal number is given by

$$S = \frac{\xi f_0}{U_c} ,$$

where ξ is the axial separation, $\left|x^{(A)}-x^{(F)}\right|$, of the hydrophone centers, and τ is the time delay between the corresponding time samples in each of the time series, i.e.,

$$\tau = t_1^{(A)} - t_1^{(F)} = \ldots = t_n^{(A)} - t_n^{(F)} = \ldots = t_N^{(A)} - t_N^{(F)}.$$

At any time delay satisfying

$$\tau = \frac{\xi}{U_c}$$

the TBL space-time correlation achieves a local maximum

$$\rho_p = \exp\left[-0.7\left|\frac{\xi f_0}{U_c}\right|\right] = \exp\left[-0.7|\tau|f_0\right] .$$

Obviously, if the condition for the third central equation is to apply exactly, the space-time correlation of the TBL pressure fluctuations, for a spatial separation ξ and a time delay $\tau = \xi/U_c$, must approach closely to unity. This implies that ξ must be very much smaller than the hydrodynamic wavelength λ_h:

$$\xi << \lambda_h = \frac{U_c}{f_0} << \frac{c}{f_0} ;$$

By way of an example, the hydrodynamic wavelength when $U_c = 0.6U_\infty = 5$ m/s (i.e., $U_\infty = 8.3$ m/s = 16.2 kts), at $f_0 = 1{,}000$ Hz, is given by $\lambda_h = 5 \times 10^{-3}$ m = 5 mm.

Fortunately, the second central equation is more tolerant with respect to allowing much wider hydrophone pair separation. For example, when ξ is equal to the hydrodynamic wavelength, λ_h, also assuming that the SNR and the number of samples are very large, then $\rho_X \simeq 0.5$. Under these conditions the second central equation is very close to being exactly satisfied. In fact, for an SNR of 100 and N = 100 the left side of the equation is within 1% of the right side. This arises from the first central equation yielding in the worst case, when the noise is correlated (i.e., $\rho_N = 1$),

$$\rho_X = 0.99\ \rho_P + 0.0099$$

for a SNR of 100 (i.e., a power ratio of 100). When the hydrophones are separated by a hydrodynamic wavelength $\rho_P \simeq 0.5$, corresponding to $\rho_X \simeq 0.5049$. Furthermore, when N = 100, for $\rho_X = 0.5049$ the third central equation leads to

$$\frac{\overline{\hat{\rho}_{X|100}\ \hat{\sigma}_{X|100}^2}}{\sigma_X^2} = \left[\frac{N}{(N-1)} - \frac{2}{(N-1)\left(1+\rho_X^2\right)}\right]\rho_X$$

$$= \left[\frac{100}{99} - \frac{2}{99 \times 1.255}\right] \times 0.5049$$

$$= 0.502;$$

this approximates $\rho_p = 0.5$ to within 0.4%.

For the case where the noise background has a partial correlation coefficient ρ_N, in order to achieve on the average relatively unbiased estimates with error smaller than $\pm\varepsilon$, the SNR

$$\gamma \simeq \frac{1}{\varepsilon}\left|\frac{\rho_N - \rho_P}{\rho_P}\right| ;$$

also, the number of independent samples needed for each hydrophone channel is

$$N \gtrsim \frac{333.3}{\left[1+\left(1+2\varepsilon\right)\rho_P{}^2\right]} - 165.7 \ .$$

A couple of examples:

a. For the worst case of completely correlated noise, and a TBL space-time maximum correlation of 0.5, to achieve an average error of 1% or less requires 100 independent samples and a SNR of 100. For an uncorrelated background, the SNR requirement remains at 100. The 0.5 peak correlation would be achieved with a hydrophone pair separation of one hydrodynamic wavelength.

b. Again for completely correlated noise, and a TBL space-time maximum correlation of 0.1, to achieve an average error of 1% requires 164 independent samples and a SNR of 890. For an uncorrelated background, the SNR requirement reduces to 100. The 0.1 peak correlation would

be achieved with a hydrophone pair separation of 3.29 times the hydrodynamic wavelength.

At this point, the variance of the estimator should be derived in order to determine the fluctuation error around the mean of the estimator. If the estimator were a regular estimation case of the continuous type (see Cramer [3]) the estimation variance could be compared with the Cramer-Rao bound to determine the efficiency of the estimator. Using the definition in Cramer [3], it appears that the estimator is not sufficient; i.e., $W_{2N}\left(\underline{X}|U_c\right)$ cannot be factored as the product of $g\left(\hat{U}_c,U_c\right)>0$ and $q_{2N}(\underline{X})$, where $q_{2N}(\underline{X})$ is independent of the U_c. The Cramer-Rao bound can be satisfied only when this condition, and the condition that

$$\frac{\partial \log_e g\left(\hat{U}_c,U_c\right)}{\partial U_c} = k\left(\hat{U}_c-U_c\right)$$

(where k is independent of $\hat{U}_c$ but may depend on U_c) both are satisfied. It therefore appears that the convection velocity estimator will not be an efficient one, i.e., it will not achieve the Cramer-Rao bound. However, because of the discontinuity in Bakewell's space-time correlation function at $\xi\to 0$ or $U_c\to\infty$, the regularity assumption is open to suspicion. Indeed, one manifestation of non-regularity can be a lower variance of the estimation error than given by the Cramer-Rao bound (cf., Cramer loc. cit, page 485). In this case, another tighter greatest lower bound for all relatively unbiased estimates, over all cases (regular and non-regular), and all SNR's is given by Barankin's approach; see Swerling [4], Glove [5].

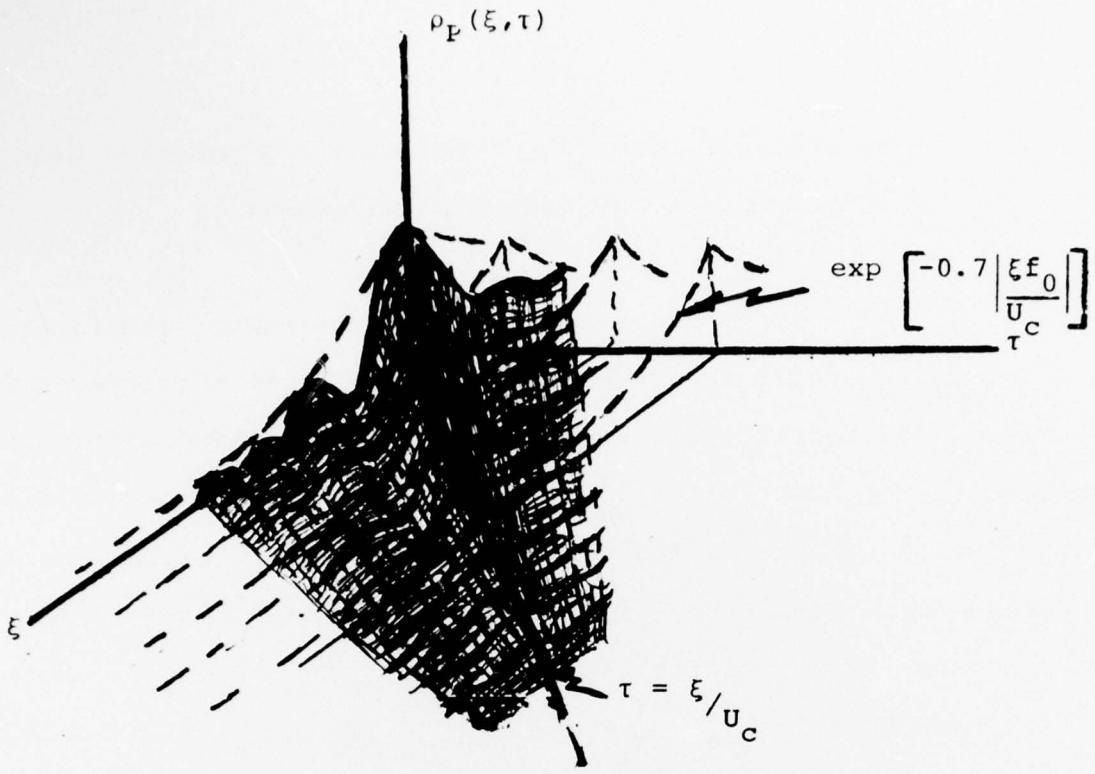

FIGURE 1: TBL SPACE-TIME CORRELATION.

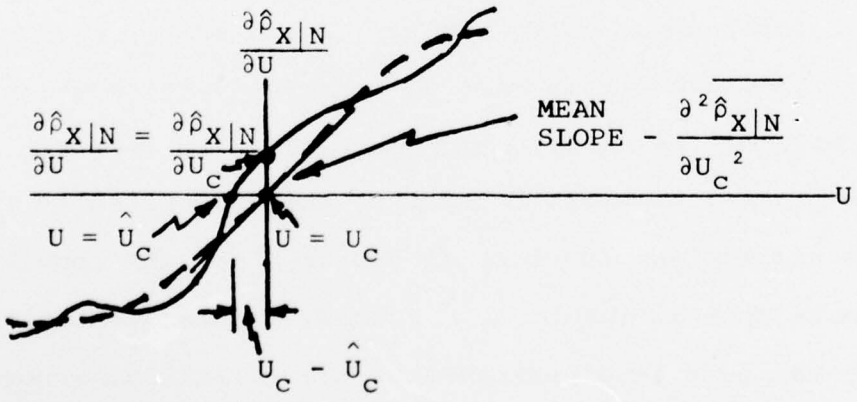

FIGURE 2: SLOPE AND ERROR GEOMETRY RELATED TO THE DERIVATIVE OF THE CORRELATION COEFFICIENT ESTIMATOR IN THE VICINITY OF $U = U_c$.

In assessing the variance of the error between the estimate, $\hat{U}_c$, of the convection velocity, and its true value, U_c, the following is appropriate. A high enough SNR is assumed such that, in the vicinity of the peak of the correlation function, no ambiguous secondary peaks occur. Moreover, for the purpose of estimating the variance, the number of samples used is assumed to be large enough to render the estimator relatively unbiased. As previously indicated, the estimated value of the convection velocity is given by the solution $U = \hat{U}_c$ to the data dependent form of the second central equation, viz:

$$\frac{\partial \hat{\rho}_{X|N}}{\partial U} = 0$$

Around the value $U = U_c$, this derivative has the mean slope

$$\left(\frac{\partial^2 \overline{\hat{\rho}_{X|N}}}{\partial U^2}\right) U = U_c$$

This is the second (i.e., linear) term in a Taylor's series expansion of the first derivative of $\hat{\rho}_{X|N}$ made around $U=U_c$. Hence, the error $\hat{U}_c - U_c$ may be written with good approximation as

$$\hat{U}_c - U_c \simeq \frac{\left(\frac{\partial \hat{\rho}_{X|N}}{\partial U}\right)}{\left(\frac{\partial^2 \overline{\hat{\rho}_{X|N}}}{\partial U^2}\right)} \begin{matrix} U = U_c \\ U = U_c \end{matrix}$$

The construction is shown graphically in Figure 2. It follows that

the variance of the error may be written as

$$\overline{\left(\hat{U}_c - U_c\right)^2} - \overline{\left(\hat{U}_c - U_c\right)}^2 = \frac{\overline{\left(\frac{\partial \hat{\rho}_{X|N}}{\partial U}\right)^2}_{U = U_c} - \left(\overline{\frac{\partial \hat{\rho}_{X|N}}{\partial U}}\right)^2_{U = U_c}}{\left(\frac{\partial^2 \overline{\hat{\rho}_{X|N}}}{\partial U^2}\right)^2_{U = U_c}}$$

However, by the theorem for differentiating products

$$\frac{\partial}{\partial U}\overline{\left[\hat{\rho}_{X|N}\,\frac{\partial \hat{\rho}_{X|N}}{\partial U}\right]} = \overline{\left(\frac{\partial \hat{\rho}_{X|N}}{\partial U}\right)^2} + \overline{\hat{\rho}_{X|N}\frac{\partial^2 \hat{\rho}_{X|N}}{\partial U^2}}$$

The term on the left vanishes because of the skew symmetric form of the product which averages to zero; also

$$\frac{\partial \hat{\rho}_{X|N}}{\partial U} = 0$$

Therefore,

$$\overline{\left(\frac{\partial \hat{\rho}_{X|N}}{\partial U}\right)^2} = -\overline{\hat{\rho}_{X|N}\frac{\partial^2 \hat{\rho}_{X|N}}{\partial U^2}}$$

Remembering that the correlation estimator $\hat{\rho}_{X|N}$ is a function of the given fixed separation, ξ, and the time-delay τ, which in turn is equal to ξ/U, it may be written as $\hat{\rho}_{X|N}(U)$. In this way;

$$-\left(\overline{\hat{\rho}_{X|N}\frac{\partial^2 \hat{\rho}_{X|N}}{\partial U^2}}\right)_{U = U_c} + \left(\overline{\hat{\rho}_{X|N}}\,\frac{\partial^2 \overline{\hat{\rho}_{X|N}}}{\partial U^2}\right)_{U = U_c}$$

maybe written as

$$-\left(\frac{\partial^2}{\partial U^2}\left[\underset{(U_c,\,U)}{\text{covar}}\ \hat{\rho}_{X|N}\right]\right)_{U\,=\,U_c}$$

where the covariance function is given by

$$\underset{(U_c,\,U)}{\text{covar}}\ \hat{\rho}_{X|N} = \overline{\hat{\rho}_{X|N}(U_c)\ \hat{\rho}_{X|N}(U)} - \overline{\hat{\rho}_{X|N}(U_c)}\ \overline{\hat{\rho}_{X|N}(U)}$$

Hence, the variance of the error in estimating the convection velocity may be written approximately as

$$\text{var}\left(\hat{U}_c - U_c\right) = -\frac{\overline{\left(\frac{\partial^2}{\partial U^2}\left[\underset{(U_c,\,U)}{\text{covar}}\ \hat{\rho}_{X|N}\right]\right)_{U\,=\,U_c}}}{\left(\frac{\partial^2}{\partial U^2}\,\overline{\hat{\rho}_{X|N}}\right)^2_{U\,=\,U_c}};$$

dimensionally, this will be the square of a velocity as

$\overline{\hat{\rho}_{X|N}}$ and $\underset{(U_c,\,U)}{\text{covar}}\ \hat{\rho}_{X|N}$ are numbers.

Returning to the definition of $\hat{\rho}_{X|N}$, namely,

$$\hat{\rho}_{X|N}(U)\,\hat{\sigma}_{X|N}^2 = \frac{1}{(N-1)}\sum_{n=1}^{N} X_n^{(F)}(U)\ X_n^{(A)}(U),$$

in order to highlight the functional dependency on ξ as well as U, it may be written in the two-dimensional form

$$\hat{\rho}_{X|N}\left(\xi,\tau\,|\,U_c\right)\hat{\sigma}_{X|N}^2 = \frac{1}{(N-1)}\sum_{n=1}^{N} X\left(x,t_m\,|\,U_c\right)\ X\left(x+\xi,t_m+\tau\,|\,U_c\right);$$

where the conditionality on U_c indicates that the actual convection velocity is given by U_c. Using this notation, the covariance of $\hat{\rho}_{X|N}$ may be expressed as

$$\underset{(U_c, U)}{\text{covar}}\ \hat{\rho}_{X|N} = \overline{\hat{\beta}_{X|N}\left(\xi, \frac{\xi}{U_c} \middle| U_c\right)\ \hat{\rho}_{X|N}\left(\xi, \frac{\xi}{U} \middle| U_c\right)} - \overline{\hat{\rho}_{X|N}\left(\xi, \frac{\xi}{U_c} \middle| U_c\right)}\ \overline{\hat{\rho}_{X|N}\left(\xi, \frac{\xi}{U} \middle| U_c\right)}.$$

It is assumed that, under a steady-flow situation, the pressure fluctuations of the TBL sensed by the hydrophones are represented by temporally stationary, spatially homogeneous Gaussian processes. Moreover, the broad-band noise fluctuations corrupting the observations also are considered as represented in a similar way. The space-time correlation (normalized) structure of the TBL pressure fluctuating field is considered to be in accord with the fifth central equation. Furthermore, the hydrophone spacing, ξ, will be comparable with a hydrodynamic wavelength, which, in the range of convection velocities under consideration, is very much smaller than an acoustic wavelength. For this reason, the corrupting noise field may be considered as completely spatially correlated. In which case, the normalized space-time correlation coefficient for the noise fluctuations in a band of width W centered around a frequency f_0 is given by

$$\rho_N(\xi,\tau) \simeq \frac{\sin[\pi W\tau]}{[\pi W\tau]} \cos[2\pi f_0 \tau].$$

Under the above conditions, it is shown in appendix A that the variance of the estimation error is given by the horrendous but dimensionally correct and intuitively satisfying equation

$$\text{var}\left(\hat{U}_c - U_c\right) = \left\{ U_c^4 \xi^2 \left[\left(2\pi f_0\right)^2 + (1/3)(\pi W)^2\right] \times \left[(1+\gamma^{-1})^2 + \exp\left(-1.4\left|\frac{\xi f_0}{U_c}\right|\right) + \gamma^{-1} \exp\left(-0.7\left|\frac{\xi f_0}{U_c}\right|\right) \frac{\sin\left(\frac{\pi W \xi}{U_c}\right)}{\left(\frac{\pi W \xi}{U_c}\right)} \cos\left(\frac{2\pi f_0 \xi}{U_c}\right)\right] + \gamma^{-1} U_c^4 \xi^2 \left[\left(\left(2\pi f_0\right)^2 + (\pi W)^2 - 2\left(\frac{U_c}{\xi}\right)^2 \frac{\sin\left(\frac{\pi W \xi}{U_c}\right)}{\left(\frac{\pi W \xi}{U_c}\right)} \cos\left(\frac{2\pi f_0 \xi}{U_c}\right)\right)\right.$$

$$+\left(4\pi^2 f_0 W\right)\frac{\cos\left(\frac{\pi W\xi}{U_c}\right)}{\left(\frac{\pi W\xi}{U_c}\right)}\sin\left(\frac{2\pi f_0\xi}{U_c}\right) - \left(\frac{4\pi f_0 U_c}{\xi}\right)\frac{\sin\left(\frac{\pi W\xi}{U_c}\right)}{\left(\frac{\pi W\xi}{U_c}\right)}\sin\left(\frac{2\pi f_0\xi}{U_c}\right)$$

$$+\left(\frac{2\pi W U_c}{\xi}\right)\frac{\cos\left(\frac{\pi W\xi}{U_c}\right)}{\left(\frac{\pi W\xi}{U_c}\right)}\cos\left(\frac{2\pi f_0\xi}{U_c}\right)\Bigg] \times \left[\exp\left(-0.7\left|\frac{\xi f_0}{U_c}\right|\right)\right.$$

$$\left.+\gamma^{-1}\frac{\sin\left(\frac{\pi W\xi}{U_c}\right)}{\left(\frac{\pi W\xi}{U_c}\right)}\cos\left(\frac{2\pi f_0\xi}{U_c}\right)\right]$$

$$+2\gamma^{-1}U_c{}^5\xi\left[\left(2\pi f_0\right)\frac{\sin\left(\frac{\pi W\xi}{U_c}\right)}{\left(\frac{\pi W\xi}{U_c}\right)}\sin\left(\frac{2\pi f_0\xi}{U_c}\right) - (\pi W)\frac{\cos\left(\frac{\pi W\xi}{U_c}\right)}{\left(\frac{\pi W\xi}{U_c}\right)}\cos\left(\frac{2\pi f_0\xi}{U_c}\right)\right.$$

$$\left.+\left(\frac{U_c}{\xi}\right)\frac{\sin\left(\frac{\pi W\xi}{U_c}\right)}{\left(\frac{\pi W\xi}{U_c}\right)}\cos\left(\frac{2\pi f_0\xi}{U_c}\right)\right] \times \left[\exp\left(-0.7\left|\frac{\xi f_0}{U_c}\right|\right)\right.$$

$$\left.\left.+\gamma^{-1}\frac{\sin\left(\frac{\pi W\xi}{U_c}\right)}{\left(\frac{\pi W\xi}{U_c}\right)}\cos\left(\frac{2\pi f_0\xi}{U_c}\right)\right]\right\}$$

$$\div N\left\{\xi^2\left[\left(2\pi f_0\right)^2 + (1/3)(\pi W)^2\right] \times \left[\exp\left(-0.7\left|\frac{\xi f_0}{U_c}\right|\right)\right]\right.$$

$$\left.+\gamma^{-1}\xi^2\left[\left(\left(2\pi f_0\right)^2 + (\pi W)^2 - 2\left(\frac{U_c}{\xi}\right)^2\right)\frac{\sin\left(\frac{\pi W\xi}{U_c}\right)}{\left(\frac{\pi W\xi}{U_c}\right)}\cos\left(\frac{2\pi f_0\xi}{U_c}\right)\right.\right.$$

$$+\left(4\pi^2 f_0 W\right)\frac{\cos\left(\frac{\pi W\xi}{U_c}\right)}{\left(\frac{\pi W\xi}{U_c}\right)}\sin\left(\frac{2\pi f_0\xi}{U_c}\right)-\left(\frac{4\pi f_0 U_c}{\xi}\right)\frac{\sin\left(\frac{\pi W\xi}{U_c}\right)}{\left(\frac{\pi W\xi}{U_c}\right)}\sin\left(\frac{2\pi f_0\xi}{U_c}\right)$$

$$+\left(\frac{2\pi W U_c}{\xi}\right)\frac{\cos\left(\frac{\pi W\xi}{U_c}\right)}{\left(\frac{\pi W\xi}{U_c}\right)}\cos\left(\frac{2\pi f_0\xi}{U_c}\right)\Bigg]$$

$$+2\gamma^{-1}U_c\xi\left[\left(2\pi f_0\right)\frac{\sin\left(\frac{\pi W\xi}{U_c}\right)}{\left(\frac{\pi W\xi}{U_c}\right)}\sin\left(\frac{2\pi f_0\xi}{U_c}\right)-(\pi W)\frac{\cos\left(\frac{\pi W\xi}{U_c}\right)}{\left(\frac{\pi W\xi}{U_c}\right)}\cos\left(\frac{2\pi f_0\xi}{U_c}\right)\right.$$

$$\left.+\left(\frac{U_c}{\xi}\right)\frac{\sin\left(\frac{\pi W\xi}{U_c}\right)}{\left(\frac{\pi W\xi}{U_c}\right)}\cos\left(\frac{2\pi f_0\xi}{U_c}\right)\right]\Bigg\}^2$$; this is the sixth central equation.

In the case where the SNR is very high (i.e., γ^{-1} becomes very small), this central equation reduces to

$$\mathrm{var}\left(\hat{U}_c - U_c\right) = \left\{\frac{U_c^4}{N\xi^2\left[\left(2\pi f_0\right)^2 + (1/3)(\pi W)^2\right]}\right\}\left[1 + \exp\left(1.4\left|\frac{\xi f_0}{U_c}\right|\right)\right]$$

In the above central equation, $\left[\left(2\pi f_0\right)^2 + (1/3)(\pi W)^2\right]$ is a measure of second moment of the power spectral density of the pressure fluctuations. As such, it is a measure of (equivalent angular-frequency bandwidth)^2. It includes the fact that a bandpass region of width W centered around f_0 is considered. If f_0 is made too large relative to W (i.e., narrow band measurements of the TBL pressure fluctuations are extracted), the space-time correlation function will exhibit a discernible quasi-periodic structure possessing ambiguous peaks which nearly compete with the central peak in determining the extraction of an estimate of U_c. To avoid this situation, the bandwidth ratio, f_0/W, of the broad-

band TBL pressure fluctuations should be no greater than 3/4. This extreme situation illustrating the secondary peaks of the space-time correlation coefficient is shown in Figure 3. In fact, inasmuch as the lower-frequency region of a towed array hydrophone output usually is dominated by low-wavenumber energy induced by vibration coupling and module scattering, it is prudent, anyway, to provide a low-pass cutoff at the bottom of the band of interest. Likewise, beyond some upper frequency determined by the boundary layer thickness, a knee occurs in the power spectral density of the TBL pressure fluctuations. Beyond this the TBL power spectral density begins to roll off at a rapid rate. Then, above this knee, even with equalization, the contribution of the TBL power would eventually be masked by the ambient noise contributions. Therefore, it would be imprudent to operate beyond some high-pass cutoff frequency determined by the anticipated boundary-layer thickness. These low- and high-pass cutoff characteristics can be made consistent with the bandwidth ratio requirement previously cited.

The central equation appropriate when the TBL pressure fluctuations dominate over the ambient noise (i.e., in the high-SNR case) then indicates that the inaccuracy due to estimation (fluctuation) noise decreases as the equivalent bandwidth increases. This may be achieved by increasing both f_0 and W consistent with the previously cited restrictions. In addition, the accuracy improves with greater hydrophone spacing but is offset through multiplication by the sum of unity and an exponential function. The optimum spacing is given by differentiating the quotient of the sum of unity and the exponential function in the numerator and ξ^2 in the denominator with respect to ξ and equating to zero. The optimum value then is given by a solution to the transcendental equation

$$-\log_e\left(0.7\left|\frac{\xi f_0}{U_c}\right| - 1\right) = 1.4\left|\frac{\xi f_0}{U_c}\right|$$

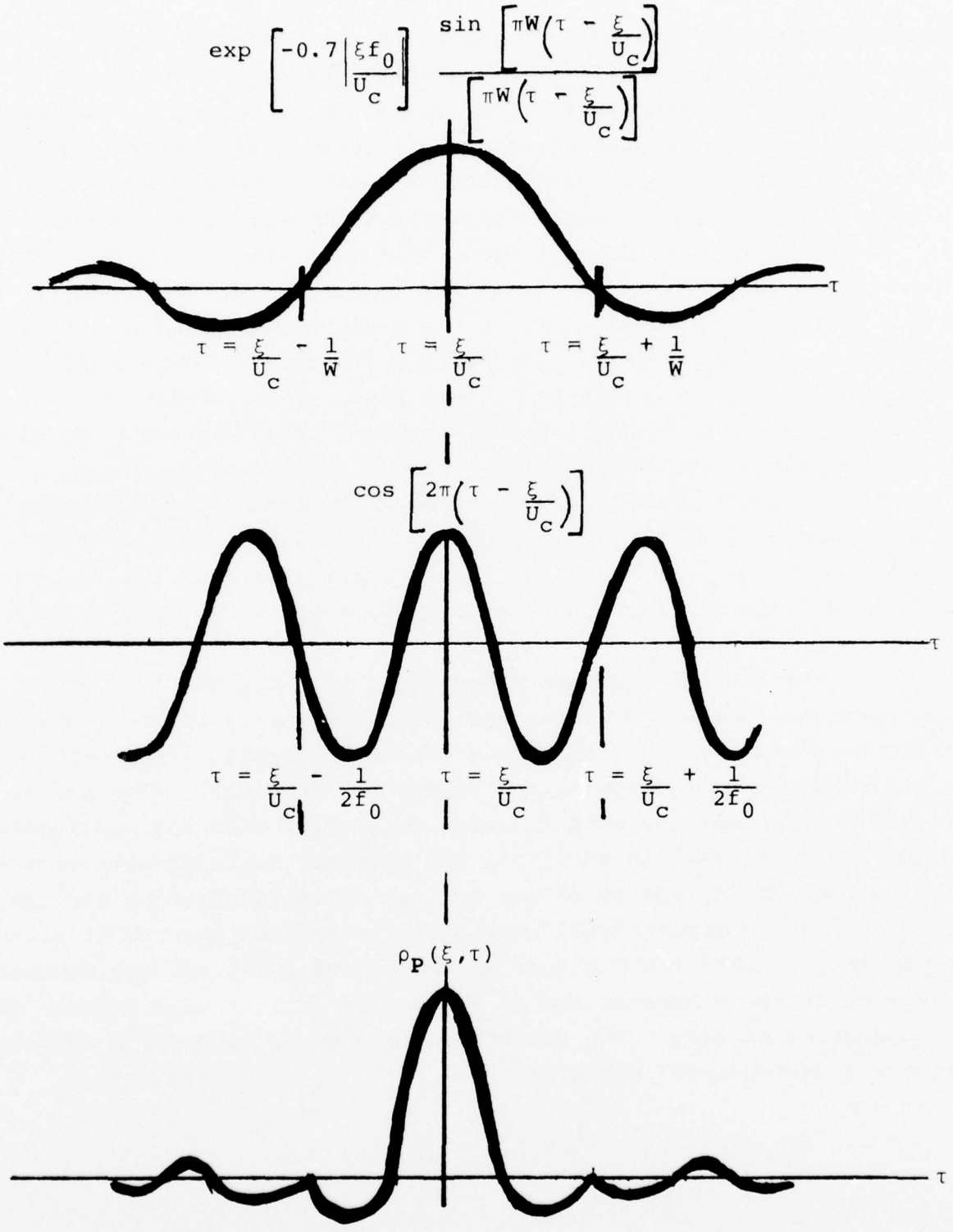

FIGURE 3: SPACE-TIME CORRELATION COEFFICIENT FOR $\frac{f_0}{W} = 3/4$.

This equation has a solution

$$\xi = \frac{1.584 U_c}{f_0} ;$$

i.e., the separation should be approximately 1.584 hydrodynamic wavelengths. In this case,

$$\mathrm{var}\left(\hat{U}_c - U_c\right) = \frac{0.1028\ U_c^2}{N\left[1 + (1/12)\left(\frac{W}{f_0}\right)^2\right]} ;$$

which, for $\frac{f_0}{W} = 3/4$, becomes

$$\mathrm{var}\left(\hat{U}_c - U_c\right) = \frac{0.0896\ U_c^2}{N}$$

or

$$\sigma\left(\hat{U}_c - U_c\right) = \frac{0.3 U_c}{\sqrt{N}} .$$

This implies that, to achieve a 1% error in the fluctuations, at least 896 independent samples are needed consistent with a hydrophone separation of $\xi = 1.584 U_c / f_0$.

Applying the optimum separation, ξ, of 1.584 hydrodynamic wavelengths and a bandwidth ratio, f_0/W, of 3/4 to the full equation for tne variance of $\left(\hat{U}_c - U_c\right)$, involving the noise as well as the TBL pressure fluctuation terms, leads to a close approximation for $\gamma \geq 10$ given by

$$\mathrm{var}\left(\hat{U}_c - U_c\right) \simeq \frac{0.0896 U_c^2}{N}\left(1+\gamma^{-1}\right)^2$$

or

$$\sigma\left(\hat{U}_c - U_c\right) \simeq \frac{0.3 U_c}{\sqrt{N}}\left(1+\gamma^{-1}\right)$$

By way of an example; with $\xi_{opt} = 1.584 \frac{U_c}{f_0}$ and $f_0/W = 3/4$ (e.g., f_0 = 1,500 Hz, W = 2,000 Hz), to achieve a Root-Mean-Square (rms) fluctuation error of 0.94% of the actual convection velocity requires about 1,000 independent samples. With the parameters chosen, $\rho_P = 0.33$, and $\rho_N = 0.05$. From previous considerations, for the bias error to be less than 0.34%,

$$N \geq \frac{333.3}{\left[1+\left(1+\frac{0.34}{50}\right)(0.33)^2\right]} - 165.7$$

or

$$N \geq 134$$

Obviously, N = 1,000 more than satisfies this lower bound. Moreover, the required SNR consistent with a bias error of 0.34% is

$$\gamma = \frac{100}{0.34}\left|\frac{0.05 - 0.33}{0.33}\right|$$

$$= 250$$

In other words, when the number of independent samples, N, and the SNR, γ, are chosen large enough consistent with a small fluctuation error, a negligible bias error is encountered. The rms addition of the bias error and the fluctuation error leads to a total error of less than ±1% of the convection velocity.

4.0 IMPLEMENTATION CONSIDERATIONS:

For a free-stream velocity, U_∞, of 16.2 kts, the convection velocity, U_c, is about 5 m/s. With f_0 set at 1,500 Hz, the hydrophone separation would have to be $\xi = 5.28 \times 10^{-3}$ m = 5.28 mm (i.e., $\xi \simeq 0.208$"). The band of frequencies being observed would be 500 Hz to 2,500 Hz. In addition, the travel time between hydrophones in the TBL would be about 10^{-3} s (i.e., 1 millisecond). To measure to within better than 1% would require a time resolution of about 10^{-5} s (i.e., 10 microseconds). To perform the processing digitally then requires a sampling rate of about 100 KHz. However, in order to decorrelate the samples in the time series derived from a hydrophone, they should be selected less frequently than about 2500 Hz (i.e., at an interval of 400 microseconds), say 2000 Hz. This would ensure that intrachannel samples did not correlate with each other. However, when the time series extracted from the forward hydrophone is time-shifted relative to the time series extracted from the aft hydrophone (see Figure 4) care must be taken to avoid inducing interchannel correlation between other samples. To avoid this artificially induced correlation, the time between samples, $(t_n - t_{n-1})$, minus the maximum anticipated time delay, $\tau = \frac{\xi}{U_c}$, must be sufficiently large so as to make the value of the space-time correlation function, $\rho_p\left(\xi, t_m - t_n + \frac{\xi}{U_c}\right)$, negligibly small for all $m \neq n$. For free-stream velocities, U_∞, down to 8 kts an intersample period of 5×10^{-3} s would suffice. In that case, in order to accumulate 1,000 independent samples, an observation period of at least 5 s would be needed. Moreover, if a Shift Register (SR) were used to achieve the time delay necessary to bring the forward hydrophone into time registra-

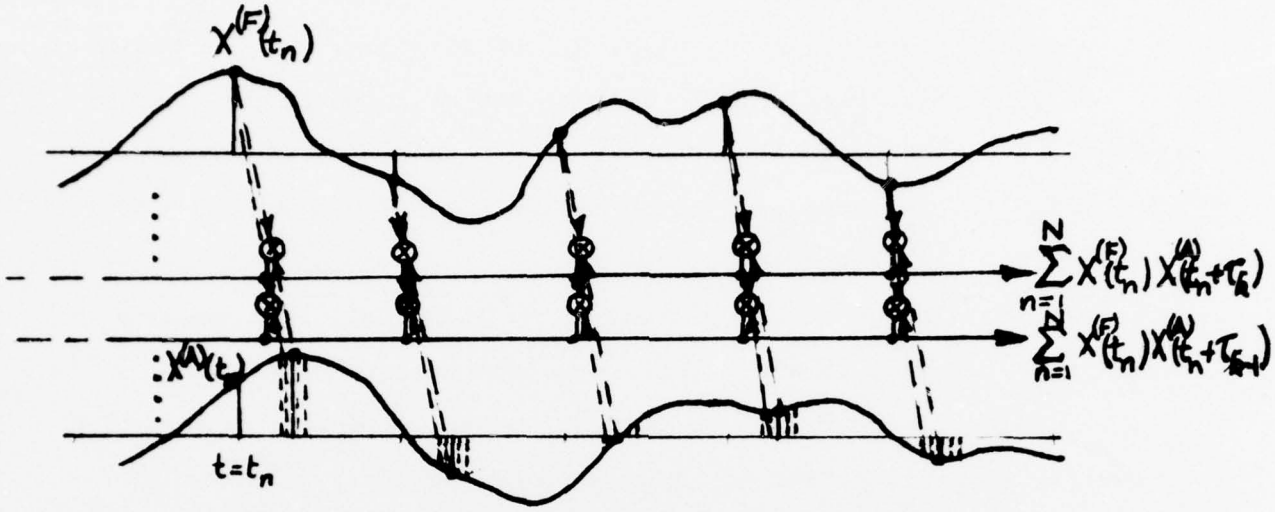

FIGURE 4: FORWARD & AFT TBL FLUCTUATION SAMPLE CROSS CORRELATION.

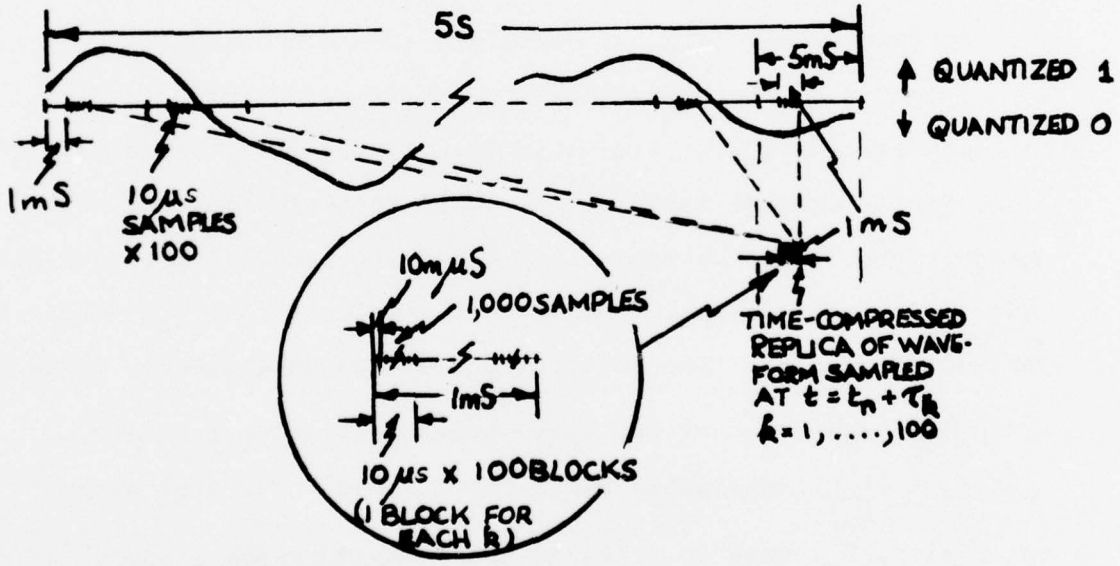

FIGURE 5a: EXAMPLE OF DELTIC TIMING FOR 100 DIFFERENT TIME DELAYS.

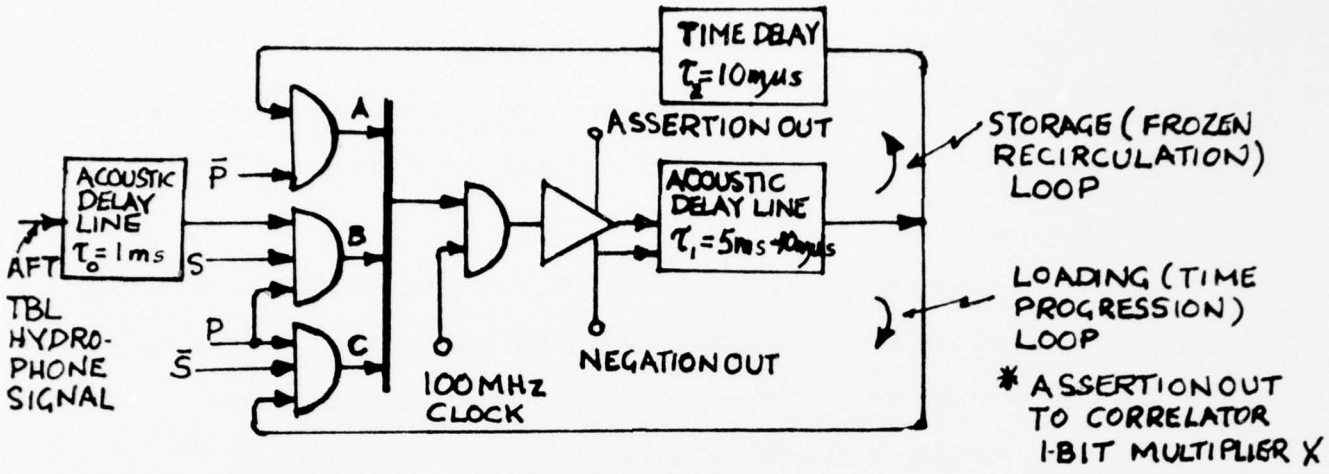

FIGURE 5b: AFT HYDROPHONE SIGNAL DELTIC

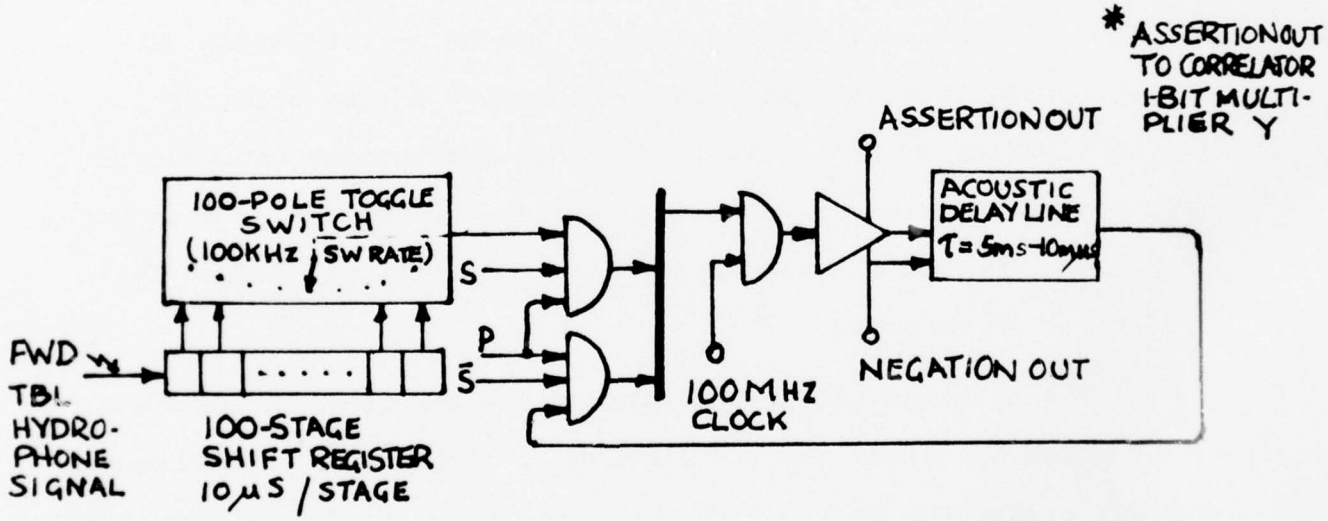

FIGURE 5c: FORWARD HYDROPHONE SIGNAL DELTIC.

tion with the aft hydrophone, at least 200 stages would be needed for a speed range down to 8 kts consistent with 1% velocity error up to 16 kts. A 2-to-1 velocity range appears to be reasonable without reoptimizing the spacing between hydrophones. The spacing should be optimized for $U_c = \sqrt{\min(U_c) \cdot \max(U_c)}$.

Inasmuch as both the TBL pressure and the noise fluctuations are broad-band, a clipper-correlator would not significantly degrade the extraction process. Either a serial DELTIC correlator or a parallel SR correlator could be used.

Figure 5 shows the correspondence needed between time samples for the DELTIC implementation. Unfortunately, in order to perform all the correlation functions with a time-delay resolution of 10^{-5}S in real time, a time speedup of 1000:1 forces clocking rates in the hundreds of MHz region. Although specialized correlators have been tested in the laboratory using, for example, a combination of Gun and charged storage diodes, in an operational device their use is not recommended.

The existing LSI technology would allow the fabrication of a miniturized processor using multistaged, tapped SR's. A schematic for performing the multiple correlations shown in Figure 4 by parallel processing is shown in Figure 6. The number of 1-bit multipliers and 10-bit up/down counters needed must match the number of tapped stages on the SR. Typically for a velocity range spanning a 2-to-1 ratio, and consistent with 1% velocity uncertainty at the highest

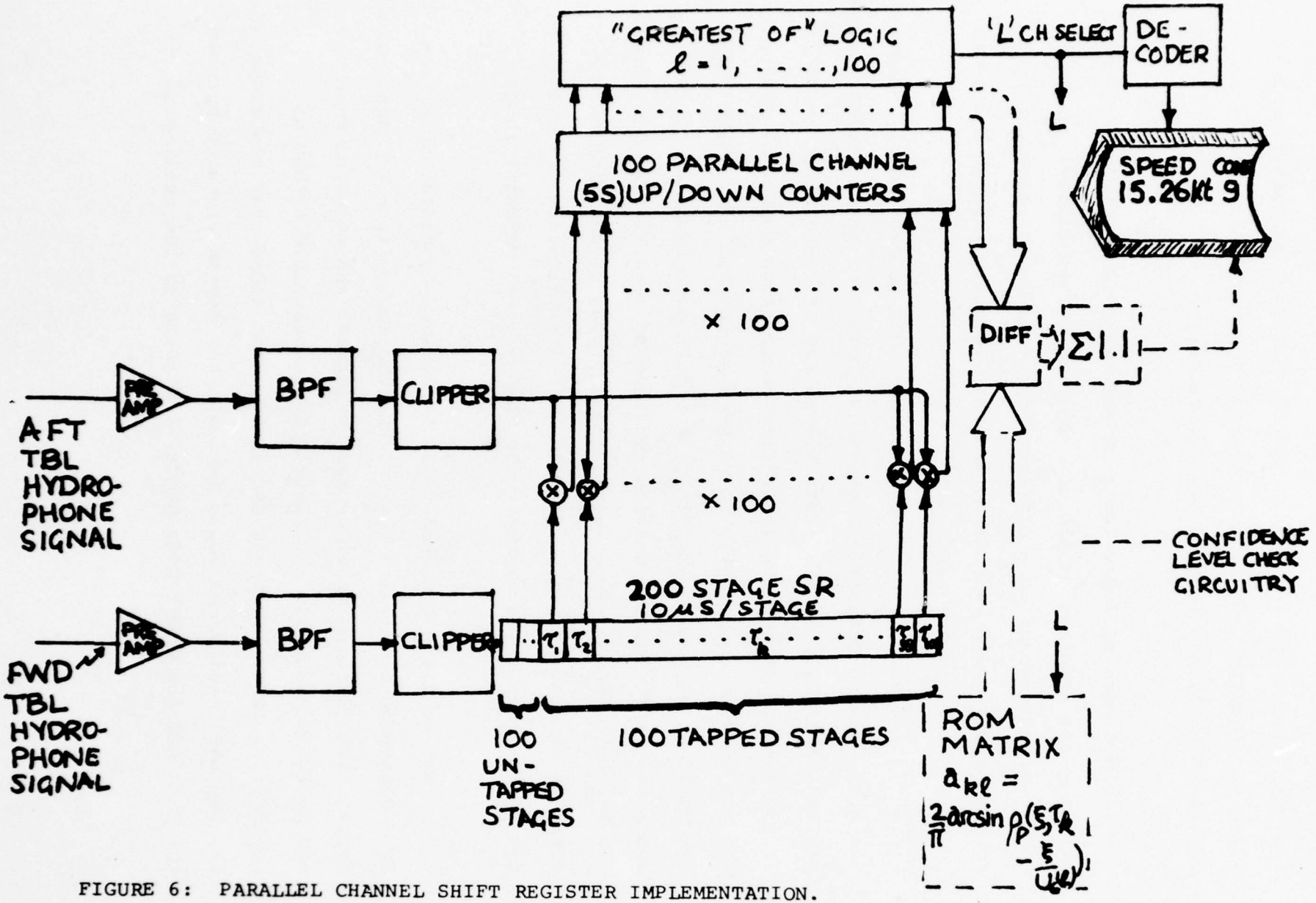

FIGURE 6: PARALLEL CHANNEL SHIFT REGISTER IMPLEMENTATION.

velocity, an SR with 200 stages and taps on the last 100 stages would be required. Thus, this form of implementation does not appear to challenge today's LSI technology.

In Figure 6, logic for peak-selecting (i.e., determining and indexing the greatest of the 100 up/down counter states) is shown. Each tap corresponds to a different free-stream velocity, so that an LED display could be made to indicate velocity through a decoder.

In addition, a confidence check could be provided by measuring the mean squared deviation between the output of the correlator on each tap, and a Read-Only Memory (ROM) stored set of correlation coefficients (i.e., a model of the TBL space-time correlation function) appropriate for the convection velocity corresponding to each tap. Namely, the ROM would store $\frac{2}{\pi}\arcsin[\rho_p(\xi_{opt}, \hat{\tau} - r\Delta)]$ corresponding to the clipped space-time correlation function centered at a particular time delay $\hat{\tau} = \xi_{opt}/\hat{U}_c$. The index, r, would ideally span either side of the correlation peak. This would require additional taps and stages on the SR in order to accommodate the whole 2-to-1 velocity range.

The confidence number would be derived by differencing the data-dependent correlator outputs and the appropriate TBL space-time correlation function model correctly indexed and selected from the ROM by the peak-selector. These differences could either be squared, or their magnitude extracted, then added over the range of r. The resultant value would indicate the degree of match between the data and the model and, hence, a measure of the quality of the

velocity estimate. This confidence level could be indicated by one digit on the LED display.

What has been described is one possible implementation of a convection (hence, free-stream) velocity indicator. The theoretical aspects of its accuracy have been analyzed, showing feasibility. Moreover, implementation is believed to be well within the state of the art.

5.0 ACKNOWLEDGMENT:

The work reported was performed under an Office of Naval Research Contract No. N00014-72-C-0318 for the Sensor Technology Program, Code 222. The authors are indebted to the encouragement and useful comments provided by Mr. H. Fitzpatrick. In addition, the authors express their gratitude for the many hours of meticulous and difficult typing provided by Mrs. E. Rees.

6.0 REFERENCES:

[1] Corcos, G.M., "Resolution of Pressure in Turbulence," JASA, Vol. 35, No. 2, February 1963.

[2] Bakewell, H.P., "Longitudinal Space-Time Correlation Function in Turbulent Airflow," JASA, Vol. 35, No. 6, July 1963.

[3] Cramer, H., Mathematical Methods of Statistics, Princeton University Press, Princeton, 1946.

[4] Swerling, P., "Parameter Estimation for Waveforms in Additive Gaussian Noise," SIAM J., Vol. 7, pp. 152-166, June 1959.

[5] Glove, F.E., "A New Look at the Barankin Lower Bound," IEEE, PGIT, Vol. IT-18, pp. 349-356, May 1972.

[6] Mohajeri, M., "A New Estimator for an Unknown Signal Imbedded in Additive Gaussian Noise," IEEE, PGIT, Vol. IT-20, No. 2, March 1974.

[7] Seidman, L.P., "Performance Limitations and Error Calculations for Parameter Estimation," Proc. IEEE, Vol. 58, pp. 664-652, May 1970.

A. APPENDICES

A.1 Deviation of the Variance of the Estimator Error

It was shown in § 3.0 that the variance of the estimator error was given by

$$\operatorname{var}\left(\hat{U}_c - U_c\right) = \frac{-\left(\frac{\partial^2}{\partial U^2} \operatorname{covar}\left(U_c, U\right) \hat{\rho}_{X|N}\right)_{U=U_c}}{\left(\frac{\partial^2}{\partial U^2} \overline{\hat{\rho}_{X|N}}\right)^2_{U=U_c}}$$

In order to evaluate the numerator and denominator of this expression, the relationship for $\hat{\rho}_{X|N}$ is recouched as

$$\hat{\rho}_{\mathbf{X}|N}(\xi,\tau) = \frac{1}{(N-1)} \sum_{n=1}^{N} X(x,t_n)\ X(x+\xi,t_n+\tau),$$

in order to highlight the spatial and temporal dependency. In this case

$$\hat{\rho}_{X|N}\left(\xi, \frac{\xi}{U_c}\right) = \frac{1}{(N-1)} \sum_{m=1}^{N} X\left(x^{(F)}, t_m\right)\ X\left(x^{(F)}+\xi, t_m+\frac{\xi}{U_c}\right)$$

and

$$\hat{\rho}_{X|N}\left(\xi, \frac{\xi}{U}\right) = \frac{1}{(N-1)} \sum_{n=1}^{N} X\left(x^{(F)}, t_n\right)\ X\left(x^{(F)}+\xi, t_n+\frac{\xi}{U}\right)$$

Thus, in evaluating the numerator of the variance of the estimator, the covariance may be written as

$$\underset{(U_c,U)}{\text{covar}}\ \hat{\rho}_{X|N} = \overline{\hat{\rho}_{X|N}\left(\xi,\frac{\xi}{U_c}\right)\hat{\rho}_{X|N}\left(\xi,\frac{\xi}{U}\right)} - \overline{\hat{\rho}_{X|N}\left(\xi,\frac{\xi}{U_c}\right)}\ \overline{\hat{\rho}_{X|N}\left(\xi,\frac{\xi}{U}\right)}$$

$$= \frac{1}{(N-1)^2}\sum_{m,n=1}^{N}\left[\overline{X\left(x^{(F)},t_m\right)X\left(x^{(F)}+\xi,t_m+\frac{\xi}{U_c}\right)X\left(x^{(F)},t_n\right)X\left(x^{(F)}+\xi,t_n+\frac{\xi}{U}\right)}\right.$$

$$\left. - \overline{X\left(x^{(F)},t_m\right)X\left(x^{(F)}+\xi,t_m+\frac{\xi}{U_c}\right)}\ \overline{X\left(x^{(F)},t_n\right)X\left(x^{(F)}+\xi,t_n+\frac{\xi}{U}\right)}\right]$$

Since all of the X(,) functions comprise the sum of two stochastic processes, P(,) and N(,), which are both Gaussianly distributed, then X(,) is Gaussianly distributed. In such case the average of the fourfold product may be replaced by the sum of three terms, each term being the product of the average of product pairs extracted from the fourfold product in cyclic order. One of these three terms cancels the negative term appearing under the double summation shown in the last equation. It follows that

$$\underset{(U_c,U)}{\text{covar}}\ \hat{\rho}_{X|N} = \frac{1}{(N-1)^2}\sum_{m,n=1}^{N}\left[\overline{X\left(x^{(F)},t_m\right)X\left(x^{(F)},t_n\right)}\ \overline{X\left(x^{(F)}+\xi,t_m+\frac{\xi}{U_c}\right)X\left(x^{(F)}+\xi,t_n+\frac{\xi}{U}\right)}\right.$$

$$\left. + \overline{X\left(x^{(F)},t_m\right)X\left(x^{(F)}+\xi,t_n+\frac{\xi}{U}\right)}\ \overline{X\left(x^{(F)},t_n\right)X\left(x^{(F)}+\xi,t_m+\frac{\xi}{U_c}\right)}\right]$$

Remembering that

$$\overline{X(x,t)\ X(x+\xi,t+\tau)} = \overline{[P(x,t)+N(x,t)][P(x+\xi,t+\tau)+N(x+\xi,t+\tau)]}$$

$$= \left[\sigma_P{}^2\rho_P(\xi,\tau) + \sigma_N{}^2\rho_N(\xi,\tau)\right],$$

as both the TBL pressure and the noise fluctuations have average zero, are assumed to be temporally stationary and spatially homogeneous, and are mutually uncorrelated, then the covariance may be expanded as

$$\underset{(U_c,U)}{\text{covar}}\,\hat{\rho}_{X|N} = \frac{1}{(N-1)^2}\sum_{m,n=1}^{N}\sum\left\{\left[\sigma_P{}^2\rho_P\left(0,t_n-t_m\right) + \sigma_N{}^2\rho_N\left(0,t_n-t_m\right)\right]\right.$$

$$\times\left[\sigma_P{}^2\rho_P\left(0,t_n-t_m+\xi\left(\frac{1}{U}-\frac{1}{U_c}\right)\right) + \sigma_N{}^2\rho_N\left(0,t_n-t_m+\xi\left(\frac{1}{U}-\frac{1}{U_c}\right)\right)\right]$$

$$+\left[\sigma_P{}^2\rho_P\left(\xi,t_n-t_m+\frac{\xi}{U}\right) + \sigma_N{}^2\rho_N\left(\xi,t_n-t_m+\frac{\xi}{U}\right)\right]$$

$$\left.\times\left[\sigma_P{}^2\rho_P\left(\xi,t_m-t_n+\frac{\xi}{U_c}\right) + \sigma_N{}^2\rho_N\left(\xi,t_m-t_n+\frac{\xi}{U_c}\right)\right]\right\}.$$

However, it must be borne in mind that the time samples were chosen so that both the TBL pressure and the noise fluctuation samples were uncorrelated intersamplewise for $t_m \neq t_n$; also the combined statistics remained identical. Therefore, only the trace terms of the double summation are nonzero. In that case,

$$\underset{(U_c,U)}{\text{covar}}\,\hat{\rho}_{X|N} = \frac{N}{(N-1)^2}\left\{\left[\sigma_P{}^2+\sigma_N{}^2\right]\left[\sigma_P{}^2\rho_P\left(0,\xi\left(\frac{1}{U}-\frac{1}{U_c}\right)\right) + \sigma_N{}^2\rho_N\left(0,\xi\left(\frac{1}{U}-\frac{1}{U_c}\right)\right)\right]\right.$$

$$\left.+\left[\sigma_P{}^2\rho_P\left(\xi,\frac{\xi}{U}\right) + \sigma_N{}^2\rho_N\left(\xi,\frac{\xi}{U}\right)\right]\left[\sigma_P{}^2\rho_P\left(\xi,\frac{\xi}{U_c}\right) + \sigma_N{}^2\rho_N\left(\xi,\frac{\xi}{U_c}\right)\right]\right\}$$

Returning to the space-time structure of the TBL pressure fluctuations, namely

$$\rho_P(\xi,\tau) = \exp\left[-0.7\left|\frac{\xi f_0}{U_c}\right|\right]\frac{\sin\left[\pi W\left(\tau-\frac{\xi}{U_c}\right)\right]}{\left[\pi W\left(\tau-\frac{\xi}{U_c}\right)\right]}\cos\left[2\pi f_0\left(\tau-\frac{\xi}{U_c}\right)\right],$$

then

$$\rho_P(0,0) = 1,$$

$$\rho_P\left(0,\frac{\xi}{U}-\frac{\xi}{U_c}\right) = \frac{\sin\left[\pi W\left(\frac{1}{U}-\frac{1}{U_c}\right)\right]}{\left[\pi W\left(t-t_c\right)\right]}\cos\left[2\pi f_0\left(\frac{1}{U}-\frac{1}{U_c}\right)\right],$$

$$\rho_P\left(\xi,\frac{\xi}{U}\right) = \exp\left[-0.7\left|\frac{\xi f_0}{U_c}\right|\right]\ \rho_P\left(0,\frac{\xi}{U}-\frac{\xi}{U_c}\right),$$

and

$$\rho_P\left(\xi,\frac{\xi}{U_c}\right) = \exp\left[-0.7\left|\frac{\xi f_0}{U_c}\right|\right].$$

Moreover, for ξ small compared with an acoustic wavelength (In § 3.0 it is shown that an optimum choice for ξ is 1.584 hydrodynamic wavelengths; a hydrodynamic wavelength, λ_h, being very much smaller than an acoustic wavelength, λ_a, for low Mach number flow.) the space-time structure of band-limited noise (of bandwidth W centered around frequency f_0) is given with good approximation by

$$\rho_N(\xi,\tau) \quad \frac{\mathrm{Sin}[\pi W\tau]}{[\pi W\tau]}\cos\,[2\pi f_0\tau],$$

$$\xi << \min\,\lambda_a = \frac{C}{f_0+\frac{W}{2}}$$

Here, C is the velocity of sound, and the minimum acoustic wavelength, min λ_a, corresponds to the highest frequency in the noise band. These statements relative to the space-time structure of the noise may be interpreted as stipulating that the noise is highly spatially correlated for small hydrophone separations, ξ, irrespective of the spatial distribution of the noise field; e.g., spherically isotropic, cylindrically isotropic, etc.--in fact, any noise not arising from a mechanism similar to that generated by TBL flow. Generally, the noise corrupting the observations arises from quite different mechanisms, such as surface-wave noise or distant shipping. In such case, the previous assumption about the space-time structure of the noise is valid.

From the above, it follows that

$$\rho_N(0,0) = 1,$$

$$\rho_N\left(0, \frac{\xi}{U} - \frac{\xi}{U_c}\right) = \frac{\sin\left[\pi W \xi \left(\frac{1}{U} - \frac{1}{U_c}\right)\right]}{\left[\pi W \xi \left(\frac{1}{U} - \frac{1}{U_c}\right)\right]} \cos\left[2\pi f_0 \xi \left(\frac{1}{U} - \frac{1}{U_c}\right)\right]$$

$$\rho_N\left(\xi, \frac{\xi}{U}\right) = \frac{\sin\left[\pi W \frac{\xi}{U}\right]}{\left[\pi W \frac{\xi}{U}\right]} \cos\left[2\pi f_0 \frac{\xi}{U}\right],$$

and

$$\rho_N\left(\xi, \frac{\xi}{U_c}\right) = \frac{\sin\left[\pi W \frac{\xi}{U_c}\right]}{\left[\pi W \frac{\xi}{U_c}\right]} \cos\left[2\pi f_0 \frac{\xi}{U_c}\right].$$

Collecting terms and inserting into the numerator of the covariance expression leads to a form

$$\underset{(U_c, U)}{\text{covar}} \hat{\rho}_{X|N} = A \frac{\sin\left[\pi W \xi \left(\frac{1}{U} - \frac{1}{U_c}\right)\right]}{\left[\pi W \xi \left(\frac{1}{U} - \frac{1}{U_c}\right)\right]} \cos\left[2\pi f_0 \xi \left(\frac{1}{U} - \frac{1}{U_c}\right)\right]$$

$$+ B \frac{\sin\left[\frac{\pi W \xi}{U}\right]}{\left[\frac{\pi W \xi}{U}\right]} \cos\left[\frac{2\pi f_0 \xi}{U}\right];$$

where

$$A = \frac{N}{(N-1)^2}\left\{\left(\sigma_P+\sigma_N\right)^2 + \sigma_P{}^4 \exp\left[-1.4\left|\frac{\xi f_0}{U_c}\right|\right]\right.$$

$$\left. + \sigma_N{}^2\sigma_P{}^2 \exp\left[-0.7\left|\frac{\xi f_0}{U_c}\right|\right] \frac{\sin\left[\frac{\pi W\xi}{U_c}\right]}{\left[\frac{\pi W\xi}{U_c}\right]} \cos\left[\frac{2\pi f_0\xi}{U_c}\right]\right\}$$

and

$$B = \frac{N}{(N-1)^2}\left\{\sigma_P{}^2\sigma_N{}^2 \exp\left[-0.7\left|\frac{\xi f_0}{U_c}\right|\right] + \sigma_N{}^4 \frac{\sin\left[\frac{\pi W\xi}{U_c}\right]}{\left[\frac{\pi W\xi}{U_c}\right]} \cos\left[\frac{2\pi f_0\xi}{U_c}\right]\right\}$$

Returning to the denominator of the expression for the variance of the error,

$$\overline{\hat{\rho}_{X|N}\left(\xi,\frac{\xi}{U}\right)} = \frac{N}{(N-1)}\left[\sigma_p{}^2\rho_p\left(\xi,\frac{\xi}{U}\right) + \sigma_n{}^2\rho_n\left(\xi,\frac{\xi}{U}\right)\right].$$

This may be written in the form

$$\overline{\hat{\rho}_{X|N}} = C \frac{\sin\left[\pi W\xi\left(\frac{1}{U} - \frac{1}{U_c}\right)\right]}{\left[\pi W\xi\left(\frac{1}{U} - \frac{1}{U_c}\right)\right]} \cos\left[2\pi f_0\xi\left(\frac{1}{U} - \frac{1}{U_c}\right)\right]$$

$$+ D \frac{\sin\left[\frac{\pi W\xi}{U}\right]}{\left[\frac{\pi W\xi}{U}\right]} \cos\left[\frac{2\pi f_0\xi}{U}\right];$$

where

$$C = \frac{N}{(N-1)}\left\{\sigma_P{}^2 \exp\left[-0.7\left|\frac{\xi f_0}{U_c}\right|\right]\right\}$$

and

$$D = \frac{N}{(N-1)} \sigma_N^2 .$$

This is the same generic form as the covariance term. Therefore, the general expressions to be doubly differentiated with-respect-to U are

$$f_1(U) = \frac{\sin\left[\pi W \xi\left(\frac{1}{U} - \frac{1}{U_c}\right)\right]}{\left[\pi W \xi\left(\frac{1}{U} - \frac{1}{U_c}\right)\right]} \cos\left[2\pi f_0 \xi\left(\frac{1}{U} - \frac{1}{U_c}\right)\right]$$

and

$$f_2(U) = \frac{\sin\left[\pi W \xi\left(\frac{1}{U}\right)\right]}{\left[\pi W \xi\left(\frac{1}{U}\right)\right]} \cos\left[2\pi f_0 \xi\left(\frac{1}{U}\right)\right] .$$

These forms may be reduced further to one canonical form by substitutions

$$u_1 = \xi\left(\frac{1}{U} - \frac{1}{U_c}\right)$$

and

$$u_2 = \xi\left(\frac{1}{U}\right) ,$$

respectively. The canonical form then becomes

$$f(u) = \frac{\sin[\pi W u]}{[\pi W u]} \cos\left[2\pi f_0 u\right] ;$$

where u can take on the value u_1 or u_2.

In either case,

$$\frac{\partial^2 f(u)}{\partial U^2} = \frac{2\xi}{U^3} \frac{\partial f(u)}{\partial u} + \frac{\xi^2}{U^4} \frac{\partial^2 f(u)}{\partial u^2} .$$

As $U \to U_c$, $u_1 \to 0$, and $u_2 \to \frac{\xi}{U_c}$. It then follows that

$$\mathrm{var}\left(\hat{U}_c - U_c\right) = \lim_{U \to U_c} \left\{ \frac{-\frac{\partial^2}{\partial U^2}\left[Af_1(U) + Bf_2(U)\right]}{\left(\frac{\partial^2}{\partial U^2}\left[Cf_1(U) + Df_2(U)\right]\right)^2} \right\}$$

$$= \lim_{\substack{u_1 \to 0 \\ u_2 \to \frac{\xi}{U_c}}} \left\{ \frac{-\frac{2\xi A}{U_c^3}\frac{\partial f(u_1)}{\partial u_1} - \frac{\xi^2 A}{U_c^4}\frac{\partial^2 f(u_1)}{\partial u_1^2} - \frac{2\xi B}{U_c^3}\frac{\partial f(u_2)}{\partial u_2} - \frac{\xi^2 B}{U_c^4}\frac{\partial^2 f(u_2)}{\partial u_2^2}}{\left(\frac{2\xi C}{U_c^3}\frac{\partial f(u_1)}{\partial u_1} + \frac{\xi^2 C}{U_c^4}\frac{\partial^2 f(u_1)}{\partial u_1^2} + \frac{2\xi D}{U_c^3}\frac{\partial f(u_2)}{\partial u_2} + \frac{\xi^2 D}{U^4}\frac{\partial^2 f(u_2)}{\partial u_2^2}\right)^2} \right\}$$

Now,

$$\lim_{u_1 \to 0} \frac{\partial f(u_1)}{\partial u_1} = 0,$$

and

$$\lim_{u_1 \to 0} \frac{\partial^2 f(u_1)}{\partial u_1^2} = -\left(2\pi f_0\right)^2 - (1/3)(\pi W)^2.$$

This second limit is a measure of the second central frequency moment of the power spectral density of the TBL fluctuations, as such is is a measure of the equivalent angular-frequency bandwidth squared. Furthermore,

$$\lim_{u_2 \to \frac{\xi}{U_c}} \frac{\partial f(u_2)}{\partial u_2} = -2\pi f_0 \frac{\sin\left[\frac{\pi W \xi}{U_c}\right]}{\left[\frac{\pi W \xi}{U_c}\right]} \sin\left[\frac{2\pi f_0 \xi}{U_c}\right]$$

$$+ \pi W \frac{\cos\left[\frac{\pi W \xi}{U_c}\right]}{\left[\frac{\pi W \xi}{U_c}\right]} \cos\left[\frac{2\pi f_0 \xi}{U_c}\right]$$

$$- \frac{U_c}{\xi} \frac{\sin\left[\frac{\pi W \xi}{U_c}\right]}{\left[\frac{\pi W \xi}{U_c}\right]} \cos\left[\frac{2\pi f_0 \xi}{U_c}\right],$$

and

$$\lim_{u_2 \to \frac{\xi}{U_c}} \frac{\partial^2 f(u_2)}{\partial u_2^2} = -\left[\left(2\pi f_0\right)^2 + (\pi W)^2 - 2\left(\frac{U_c}{\xi}\right)^2\right] \times \frac{\sin\left[\frac{\pi W \xi}{U_c}\right]}{\left[\frac{\pi W \xi}{U_c}\right]} \cos\left[\frac{2\pi f_0 \xi}{U_c}\right]$$

$$- 4\pi^2 f_0 W \frac{\cos\left[\frac{\pi W \xi}{U_c}\right]}{\left[\frac{\pi W \xi}{U_c}\right]} \sin\left[\frac{2\pi f_0 \xi}{U_c}\right]$$

$$+ \frac{4\pi f_0 U_c}{\xi} \frac{\sin\left[\frac{\pi W \xi}{U_c}\right]}{\left[\frac{\pi W \xi}{U_c}\right]} \sin\left[\frac{2\pi f_0 \xi}{U_c}\right]$$

$$- \frac{2\pi W U_c}{\xi} \frac{\cos\left[\frac{\pi W \xi}{U_c}\right]}{\left[\frac{\pi W \xi}{U_c}\right]} \cos\left[\frac{2\pi f_0 \xi}{U_c}\right].$$

These equations are combined in all their glory to provide a general expression for the variance of the estimator error in §3.0. As a checkpoint, the case for $\sigma_N^2 = 0$ (i.e., infinite SNR) is examined. Then,

$$\mathrm{var}\left(\hat{U}_c - U_c\right) = \frac{U_c^4 \left\{1 + \exp\left[1.4 \left|\frac{\xi f_0}{U_c}\right|\right]\right\}}{N\xi^2 \left[\left(2\pi f_0\right)^2 + (1/3)(\pi W)^2\right]}$$

or

$$\sigma\left(\hat{U}_c - U_c\right) = \frac{U_c^2\left\{1+\exp\left[1.4\left|\frac{\xi f_0}{U_c}\right|\right]\right\}^{1/2}}{N^{1/2}\xi\left[\left(2\pi f_0\right)^2 + (1/3)(\pi W)^2\right]^{1/2}} .$$

The interpretation of the latter form is that the rms error varies inversely as the square root of the number of independent samples used in assembling an estimate of U_c. It decreases as the equivalent angular-frequency bandwidth

$$\left[\left(2\pi f_0\right)^2 + (1/3)(\pi W)^2\right]^{1/2}$$

increases. It further decreases initially with an increase in the hydrophone separation, ξ, but eventually reaches a minimum, its decrease being overtaken by the factor

$$\left\{1+\exp\left[1.4\left|\frac{\xi f_0}{U_c}\right|\right]\right\}^{1/2} .$$

In §3.0 it is shown that the minimum occurs when

$$\xi = 1.584\ \frac{U_c}{f_0} \stackrel{\text{Def}}{=} \xi_{opt.}$$

The rms error also is proportional to the actual value of the convection velocity, U_c, squared. However, one of the U_c's in the squared quantity matches dimensionally with the product of ξ and the equivalent bandwidth. When the optimum separation, ξ_{opt}, is used, one of these U_c's cancels, and the rms error then is directly proportional to U_c.

If the band in which the TBL pressure fluctuations are observed is too narrow, competing secondary peaks evince themselves in the space-time correlation function. These secondary peaks cause

ambiguities in locating the peak of the correlation, which the MLE indicates to be the optimum way in which to estimate U_c. In order to avoid this undesirable effect, the observation frequency band should be sufficiently wide. In §3.0 a rationale is constructed for choosing a value of bandwidth ratio f_0/W equal to 3/4.

A.2 Deviation of the Bias Error

From the development in §3.0, the bias error was given by

$$b\left(U_c\right) = \bar{\hat{U}}_c - U_c$$

$$= \frac{\left(\frac{\partial \bar{\hat{\rho}}_{X|N}}{\partial U}\right)_{U = U_c}}{\left(\frac{\partial^2 \bar{\hat{\rho}}_{X|N}}{\partial U^2}\right)_{U = U_c}}$$

Using the equations developed in Appendix A.1,

$$b\left(U_c\right) = \lim_{\substack{u_1 \to 0 \\ u_2 \to \frac{\xi}{U_c}}} \left\{ \frac{-\frac{C\xi}{U_c^2}\frac{\partial f\left(u_1\right)}{\partial u_1} - \frac{D\xi}{U_c^2}\frac{\partial f\left(u_2\right)}{\partial U_2}}{\frac{2\xi C}{U_c^3}\frac{\partial f\left(u_1\right)}{\partial u_1} + \frac{\xi^2 C}{U_c^4}\frac{\partial^2 f\left(u_1\right)}{\partial u_1^2} + \frac{2\xi D}{U_c^3}\frac{\partial f\left(u_2\right)}{\partial u_2} + \frac{\xi^2 D}{U^4}\frac{\partial^2 f\left(u_2\right)}{\partial u_2^2}} \right\}$$

This may be written

$$b\left(U_c\right) = U_c \gamma^{-1} \left\{ \frac{2\pi f_0 \xi}{U_c} \frac{\sin\left[\frac{\pi W \xi}{U_c}\right]}{\left[\frac{\pi W \xi}{U_c}\right]} \sin\left[\frac{2\pi f_0 \xi}{U_c}\right] + \left[\frac{\sin\left[\frac{\pi W \xi}{U_c}\right]}{\left[\frac{\pi W \xi}{U_c}\right]} - \cos\left[\frac{\pi W \xi}{U_c}\right] \right] \cos\left[\frac{2\pi f_0 \xi}{U_c}\right] \right\}$$

$$\div\left\{\frac{\xi^2}{U_c^2}\left[\left(2\pi f_0\right)^2 + (1/3)(\pi W)^2\right] \times \left[\exp\left(-0.7\left|\frac{\xi f_0}{U_c}\right|\right)\right]\right.$$

$$+\gamma^{-1}\frac{\xi^2}{U_c^2}\left[\left(\left(2\pi f_0\right)^2 + (\pi W)^2 - 2\left(\frac{U_c}{\xi}\right)^2\right)\frac{\sin\left(\frac{\pi W\xi}{U_c}\right)}{\left(\frac{\pi W\xi}{U_c}\right)}\cos\left(\frac{2\pi f_0\xi}{U_c}\right)\right.$$

$$+\left(4\pi^2 f_0 W\right)\frac{\cos\left(\frac{\pi W\xi}{U_c}\right)}{\left(\frac{\pi W\xi}{U_c}\right)}\sin\left(\frac{2\pi f_0\xi}{U_c}\right) - \left(\frac{4\pi f_0 U_c}{\xi}\right)\frac{\sin\left(\frac{\pi W\xi}{U_c}\right)}{\left(\frac{\pi W\xi}{U_c}\right)}\sin\left(\frac{2\pi f_0\xi}{U_c}\right)$$

$$\left.+\left(\frac{2\pi W U_c}{\xi}\right)\frac{\cos\left(\frac{\pi W\xi}{U_c}\right)}{\left(\frac{\pi W\xi}{U_c}\right)}\cos\left(\frac{2\pi f_0\xi}{U_c}\right)\right]$$

$$+2\gamma^{-1}\frac{\xi}{U_c}\left[\left(2\pi f_0\right)\frac{\sin\left(\frac{\pi W\xi}{U_c}\right)}{\left(\frac{\pi W\xi}{U_c}\right)}\sin\left(\frac{2\pi f_0\xi}{U_c}\right) - (\pi W)\frac{\cos\left(\frac{\pi W\xi}{U_c}\right)}{\left(\frac{\pi W\xi}{U_c}\right)}\cos\left(\frac{2\pi f_0\xi}{U_c}\right)\right.$$

$$\left.\left.+\left(\frac{U_c}{\xi}\right)\frac{\sin\left(\frac{\pi W\xi}{U_c}\right)}{\left(\frac{\pi W\xi}{U_c}\right)}\cos\left(\frac{2\pi f_0\xi}{U_c}\right)\right]\right\} .$$

This is the central equation determining the bias error.

As may be seen, the bias error vanishes as the SNR becomes large, and the estimator becomes unbiased. For the values of γ and N derived from the equations in §3.0, the bias error fraction $b\left(U_c\right)/U_c$ becomes negligibly small. In fact, once a value of N is chosen to

make the variance of the estimator (i.e., fluctuation) error acceptably low, this value usually is more than adequate for SNR's in the order of 100 or more to guarantee a bias error negligible in comparison with the fluctuation error.

A.3 Cramer-Rao Bound on Convection Velocity MLE

The Cramer-Rao (CR) bound provides a lower bound on the minimum variance of the estimator error. Although not always achieved, it serves as a measure of the ultimate in accuracy that may be achieved under an MLE. When the achievable variance of the estimator error is compared with the CR bound, a measure of the efficiency of the estimator is derived. In some cases, the CR is achieved as the number of samples, N, tends to infinity, in which case the bound is said to be asymptotically efficient.

In the notation of §3.0, the CR bound may be written as

$$\mathrm{Var}\left(\hat{U}_c - U_c\right) \geq \frac{\left[1 + \frac{\partial b\left(U_c\right)}{\partial U_c}\right]^2}{\int_{-\infty}^{+\infty} \cdots \int \left(\frac{\partial}{\partial U_c} \log_e \left[W_{2N}\left(\underline{X} \mid U_c\right)\right]\right)^2 W_{2N}\left(\underline{X} \mid U_c\right) d^N \underline{X}}$$

or

$$\mathrm{Var}\left(\hat{U}_c - U_c\right) \geq \frac{\left[1 + \frac{\partial b\left(U_c\right)}{\partial U_c}\right]^2}{E\left\{\left(\frac{\partial}{\partial U_c} \log_e \left[W_{2N}\left(\underline{X} \mid U_c\right)\right]\right)^2\right\}};$$

where $E\{ \cdot \}$ connotes the expected value of the quantity within the braces, and $b\left(U_c\right)$ is the bias-error given by $b\left(U_c\right) = E\left(\hat{U}_c\right) - U_c$. For an unbiased estimator, $b\left(U_c\right)$ is zero.

Returning to §3.0, the partial derivative of the natural logarithum of the likelihood function reduces to

$$\frac{\partial}{\partial U_c}\log_e\left[W_{2N}\left(\underline{X}|U_c\right)\right] = -\frac{\partial}{\partial U_c}\left\{\rho_X \sum_{n=1}^{N}\left[\left(X_n^{(F)}\right)^2 + \left(X_n^{(A)}\right)^2 - 2\rho_X X_n^{(F)} X_n^{(A)}\right]\right.$$

$$\left. -\left(1-\rho_X^2\right)\sum_{n=1}^{N} X_n^{(F)} X_n^{(A)} - N\rho_X\left(1-\rho_X^2\right)\sigma_X^2\right\}$$

$$\times\left[\frac{1}{\sigma_X^2\left(1-\rho_X^2\right)^2}\frac{\partial\rho_X}{\partial U_c}\right]$$

$$= -\left\{\sum_{n=1}^{N}\left[\left(X_n^{(F)}\right)^2 + \left(X_n^{(A)}\right)^2 - \left(\rho_X+\frac{1}{\rho_X}\right) X_n^{(F)} X_n^{(A)}\right]\right.$$

$$\left. - N\left(1-\rho_X^2\right)\sigma_X^2\right\}\left[\frac{\rho_X}{\sigma_X^2\left(1-\rho_X^2\right)^2}\frac{\partial\rho_X}{\partial U_c}\right]$$

As might be anticipated, the expected value of the derivative vanishes. However, this is not so for the square of each side of the equation. Indeed, after some manipulation,

$$E\left\{\left(\frac{\partial}{\partial U_c}\log_e\left[W_{2N}\left(\underline{X}|U_c\right)\right]\right)^2\right\} = E\left\{N^2\left(1-\rho_X^2\right)\sigma_X^4\right.$$

$$- 2N\left(1-\rho_X^2\right)\sigma_X^2\sum_{n=1}^{N}\left[\left(X_n^{(F)}\right)^2 + \left(X_n^{(A)}\right)^2 - \left(\rho_X+\frac{1}{\rho_X}\right) X_n^{(F)} X_n^{(A)}\right]$$

$$+ \sum_{m,n=1}^{N}\left[\left(X_m^{(F)}\right)^2 + \left(X_m^{(A)}\right)^2 - \left(\rho_X+\frac{1}{\rho_X}\right) X_m^{(F)} X_m^{(A)}\right]$$

$$\left.\times\left[\left(X_n^{(F)}\right)^2 + \left(X_n^{(A)}\right)^2 - \left(\rho_X+\frac{1}{\rho_X}\right) X_n^{(F)} X_n^{(A)}\right]\right\}$$

$$\times\left[\frac{\rho_X}{\sigma_X^2\left(1-\rho_X^2\right)^2}\frac{\partial\rho_X}{\partial U_c}\right]^2$$

becomes (using the rule for decomposing the expected value of the fourfold product of Gaussian processes into the sum of cyclic products of pair-wise products; as exploited in Appendix A.1)

$$E\left\{\left(\frac{\partial}{\partial U_c}\log_e\left[W_{2N}\left(\underline{X}|U_c\right)\right]\right)^2\right\} = \frac{N\left(1+\rho_X{}^2\right)}{\left(1-\rho_X{}^2\right)^2}\left(\frac{\partial \rho_X}{\partial U_c}\right)^2$$

The CR bound then becomes

$$\text{var}\left(\hat{U}_c - U_c\right) > \frac{\left(1-\rho_X{}^2\right)^2\left(\frac{\partial \bar{U}_c}{\partial U_c}\right)^2}{N\left(1+\rho_X{}^2\right)\left(\frac{\partial \rho_X}{U_c}\right)^2};$$

where

$$\frac{\partial \bar{U}_c}{\partial U_c} = 1 + \frac{\partial b\left(U_c\right)}{\partial U_c}$$

.

When $\gamma^{-1} \to 0$ (i.e., asymptotically high SNR), $\rho_X \to \rho_p$. The CR bound is derived without regard for the data manipulations indicated by a MLE solution. In fact, the CR bound essentially provides that, under certain conditions of regularity, a greatest lower bound exists. Other more stringent conditions such as sufficiency, and a tighter condition mentioned in §3.0, must be observed if the equality of the bound is to be satisfied. Thus, in view of the fact that the observables $\underline{X}^{(F)}$ and $\underline{X}^{(A)}$ are taken initially without knowledge that an MLE of U_c would result from deriving an estimate of the time delay $\tau = \frac{\xi}{U_c}$ which maximizes the TBL space-time correlation function, the function $\rho_p(\xi,0)$ is the one appropriate for deriving the CR bound.

Then, for $\gamma^{-1} \to 0$, using $\rho_p(\xi,0)$ and $\frac{\partial \rho_p(\xi,0)}{\partial U_c}$, and performing the indicated manipulations, a family of CR bounds may be derived for each value of the variable ξ. In fact, it is readily seen that the CR bound thus derived is not uniformly the greatest lower bound over the range of $\xi \varepsilon [0, \infty)$. A minimum value of the CR bound is found to correspond to $\frac{\xi f_0}{U_c} \simeq 0.1$; which differs markedly from the value $\frac{\xi_{opt} f_0}{U_c} \simeq 1.584$ appropriate to the minimum variance of the estimator error derived by the MLE procedure. Moreover, the value of the CR bound derived for $\frac{\xi f_0}{U_c} \simeq 0.1$ is found to be

$$\text{var}\left(\hat{U}_c - U_c\right) \geq \frac{0.7602\ U_c^2}{N}$$

as opposed to

$$\text{var}\left(\hat{U}_c - U_c\right) = \frac{0.0896\ U_c^2}{N}$$

corresponding to the MLE for a choice of $\frac{\xi_{opt} f_0}{U_c} \simeq 1.584$. Thus, the MLE procedure has resulted in a relatively unbiased estimate of "abnormally high" precision; exceeding that indicated by the CR bound!

This anomaly has been carefully checked, and a lot of time and effort was expended in chasing an illusory factor of 2π*, but the discrepancy appears to be real. Its roots most likely are involved

* A factor of 2π, as either a divisor of the CR bound or a multiplier of the MLE variance, would make the MLE of convection velocity an estimator of efficiency 2; i.e., the variance of the MLE would be twice the CR bound. As observed in §3.0, this MLE would not lead to a sufficient estimator, and an efficiency of 2 might be expected.

in the non-regularity of the PDF of the observables around the value of $\xi = 0$ or $U_c = \infty$. Indeed the Bakewell (loc. cit.) space-time correlation function has a discontinuity in the immediate neighborhood of these values. In fact, the function

$$\exp\left[-0.7\left|\frac{\xi f_0}{U_c}\right|\right]$$

entering into Bakewell's space-time correlation function corresponds to the autocorrelation function for a lst-order Markoffian (i.e., autoregressive) process when $\tau=\frac{\xi}{U_c}$. Swerling (loc. cit.), and his doctoral students, investigated other tighter bounds and estimation procedures for non-regular estimation cases; including cases concerned in estimating correlation coefficients and functions associated with seemingly innocuous problems involving lst-order Markoffian processes. This work involved the Barankin approach; see Swerling loc. cit. and Glove loc. cit. In addition, Cramer (loc. cit, page 485) alludes to similar anomalies.

Other estimation procedures and bounds have been studied, such as the c-a estimator by Mohajeri [6] and the Ziv-Zakai bound discussed in a paper by Seidman [7]. Each claims a different advantage or tighter bound under various assumptions. Nevertheless, the MLE derived in §3.0 and Appendix A.1 does have all the attributes intuitively expected of an estimator of convection velocity. Hence, for the purposes of deriving design equations and guidelines, the MLE is offered as a reasonable estimation procedure. It may not be a locally "best" unbiased estimator in the sense of the recursion techniques provided by the Barankin approach; but sufficient to the day is the rigor thereof.

DISTRIBUTION LIST

DCASMA, Garden City
605 Stewart Avenue
Garden City, L.I., N.Y. 11530
Attn: Scientific Officer-N00014 (2)
Administrative Contracting
Officer-S3309A (1)

Applied Research Laboratory
P.O. Box 30
State College, Pennsylvania 16801
Attn: Prof. B.R. Parkin, Director
Garfield Thomas Water Tunnel (1)

Mr. Hugh M. Fitzpatrick
Code 458
Office of Naval Research
Arlington, Virginia 22217 (1)

Applied Physics Laboratory
University of Washington
1013 N.E. 40th Street
Seattle, Washington 98105
Attn: Dr. W. Davis (1)

Cambridge Acoustical Associates, Inc.
1033 Massachusetts Avenue
Cambridge, Massachusetts 02138
Attn: Dr. M. Junger (1)

Commander
Naval Ship Research & Development Ctr.
Washington, D.C. 20034
Attn: Dr. D. Vendettis - 112 (1)
Dr. D. Feit - 159 (1)
Dr. A. Bisson - 232A (1)
Dr. G. Maidanik - 343 (1)
Dr. P. Rispin - 214 (1)

Commander
Naval Electronic Systems Command
PME 124-40
2511 Jefferson Davis Highway
National Center #1
Arlington, Virginia 20360
Attn: Mr. J. Hussmann (1)

General Electric Company
Heavy Military Electronic Systems
Syracuse, New York 13201 (1)

Commander
Naval Ocean Systems Center
San Diego, California 92152
Attn: Dr. R. Smith (1)

Commanding Officer
Naval Underwater Systems Center
New London Laboratory
New London, Connecticut 06320
Attn: Mr. J. Marsh (1)
Dr. H. Bakewell (1)
Dr. A. Markowitz (1)

Commanding Officer
Naval Underwater Systems Center
Central Test & Evaluation Activity
1651 SW 40th Street
Ft. Lauderdale, Florida 33315
Attn: Dr. R. Kennedy (1)

Commanding Officer
Naval Ocean Research & Development
Activity - NSTL Station
Mississippi 39529
Attn: Cmdr. G. Ranes (1)

Bolt Beranek & Newman, Inc.
50 Moulton Street
Cambridge, Massachusetts 02138 (1)

Gould Incorporated
Chesapeake Instrument Division
6711 Baymeadow Drive
Glen Burnie, Maryland 21061 (1)

Sperry-Univac
Univac Park
Mail Station No. U2K13
St. Paul, Minnesota 55165
Attn: Mr. R. Johnson (1)
Mr. Q. Heckart (1)
Mr. D. Jones (1)

MAR, Inc.
1335 Rockville Pike
Rockville, Maryland 20852 (1)

Commander
Naval Sea Systems Command
Department of the Navy
Washington, D.C. 20362
Attn: Code 06H1 (1)
Mr. T. Oliver - 06H2 (1)

Commander
Naval Electronic Systems Command
Code 320
2511 Jefferson Davis Highway
National Center #1
Arlington, Virginia 20360 (1)

DISTRIBUTION LIST (CON'T)

Hughes Aircraft Company
Ground Systems Group
1901 West Malvern Avenue
Fullerton, California 92634 (1)

Johns Hopkins University
Applied Physics Laboratory
SSBN Security Program
Johns Hopkins Road
Laurel, Maryland 20810 (1)

Raytheon Corporation
Submarine Signal Division
Portsmouth, Rhode Island 20871 (1)

General Dynamics Corporation
Electric Boat Division
Eastern Point Road
Groton, Connecticut 06340 (1)

Defense Documentation Center
Cameron Station
Alexandria, Virginia 22314 (12)

Director
Naval Research Laboratory
Code 2627
4555 Overlook Avenue S.W.
Washington, D.C. 20375 (6)

Office of Naval Research
800 N. Quincy Street
Arlington, Virginia 22217
Attn: Code 222 (2)
Code 102IP (6)

Office of Naval Research
Branch Office
495 Summer Street
Boston, Massachusetts 02210 (1)

SECURITY CLASSIFICATION OF THIS PAGE (When Data Entered)

REPORT DOCUMENTATION PAGE

READ INSTRUCTIONS BEFORE COMPLETING FORM

1. REPORT NUMBER: WB77-1	2. GOVT ACCESSION NO.
3. RECIPIENT'S CATALOG NUMBER	
4. TITLE (and Subtitle): MAXIMUM-LIKELIHOOD FLOW-SPEED ESTIMATION, [redacted]	5. TYPE OF REPORT & PERIOD COVERED: Interim Rept.
6. PERFORMING ORG. REPORT NUMBER	
7. AUTHOR(s): S. Gardner and F.L. Rees	8. CONTRACT OR GRANT NUMBER(s): N00014-72-C-0318
9. PERFORMING ORGANIZATION NAME AND ADDRESS: BINARY SYSTEMS, INC. 10750 Columbia Pike, Suite 301 Silver Spring, Md. 20901	10. PROGRAM ELEMENT, PROJECT, TASK AREA & WORK UNIT NUMBERS: 61153N, RR031-03, RR031-03-84, NR386-805
11. CONTROLLING OFFICE NAME AND ADDRESS: Sensor Technology Program, Code 222 Office of Naval Research, 800 N. Quincy Arlington, Va. 22217	12. REPORT DATE: May 24, 1977
	13. NUMBER OF PAGES: 64
14. MONITORING AGENCY NAME & ADDRESS (if different from Controlling Office)	15. SECURITY CLASS. (of this report): Unclassified
	15a. DECLASSIFICATION/DOWNGRADING SCHEDULE

16. DISTRIBUTION STATEMENT (of this Report)

Approved for public release; distribution unlimited.

17. DISTRIBUTION STATEMENT (of the abstract entered in Block 20, if different from Report)

18. SUPPLEMENTARY NOTES

19. KEY WORDS (Continue on reverse side if necessary and identify by block number)

Turbulent Boundary Layer; Pressure Fluctuations; Convection Speed; Maximum-Likelihood Estimate; TBL Cross Correlation.

20. ABSTRACT (Continue on reverse side if necessary and identify by block number)

The design formulae and theoretical performance of a maximum-likelihood estimator for towed-array flow-speed estimation are discussed. Under appropriate conditions, it is shown that a maximum-likelihood estimate of convection velocity (which is related to tow speed) is achieved by performing a cross correlation between the outputs of two streamwise-separated flush-mounted surface probe hydrophones. The estimate, then, is derived by

→ next page

DD FORM 1 JAN 73 1473 EDITION OF 1 NOV 65 IS OBSOLETE
S/N 0102-LF-014-6601

Unclassified
SECURITY CLASSIFICATION OF THIS PAGE (When Data Entered)

410409

seeking the time delay which maximizes the cross correlation.

Conditions are examined consistent with achieving accurate speed determination to within a fraction of a knot. Fortuitously, the method derived has the property that, as speed is increased, both the level and bandwidth of the pressure signals increase, thus providing increased signal-to-noise ratio and more accurate time-delay information.

It is suggested that a confidence-level measurement, comparing the space-time correlation function derived from the data with a theoretical model, could be used to indicate flow anomalies. These flow anomalies might be attributable to disturbances such as flow separation. In such case, the device could be used also to sense flow stability.

Two implementations are discussed: one using a DElay Line TIme Compressor (DELTIC) and serial processing; the other using Shift Registers (SR) and parallel processing. A trade-off of serial faster-than-real-time DELTIC processing speed requirements against the high degree of parallel processing needed with the SR approach is discussed.

A recommendation is made to design, build, and test such a speed estimation/stability sensor on standard towed arrays. It further is suggested that empirical results and experience thus derived could be extrapolated, along with a study of available other array surface pressure coherency data, to determine the feasibility of building such a sensor for non-standard towed array application.